

Study of Drug Delivery Using Purely Organic Macrocylic Containers—Cucurbit[7]uril and Pillararene

Arnab Roy Chowdhury and Soumyabrata Goswami*



Cite This: *ACS Omega* 2023, 8, 47340–47366



Read Online

ACCESS |

Metrics & More

Article Recommendations



ABSTRACT: An impaired immune system is the root of various human ailments provoking the urge to find vehicle-mediated quick delivery of small drug molecules and other vital metabolites to specific tissues and organs. Thus, drug delivery strategies are in need of improvement in therapeutic efficacy. It can be achieved only by increasing the drug-loading capacity, increasing the sustained release of a drug to its target site, easy relocation of drug molecules associated with facile complexation-induced properties of molecular vehicles, and high stimuli-responsive drug administration. Supramolecular drug delivery systems (SDDS) provide a much needed robust yet facile platform for fabricating innovative drug nanocarriers assembled by thermodynamically noncovalent interaction with the tunable framework and above-mentioned properties. Measures of cytotoxicity and biocompatibility are the two main criteria that lie at the root of any promising medicinal applications. This Review features significant advancements in (i) supramolecular host–guest complexation using cucurbit[7]uril (CB[7]), (ii) encapsulation of the drug and its delivery application tailored for CB[7], (iii) self-assembly of supramolecular amphiphiles, (iv) supramolecular guest relay using host–protein nanocavities, (v) pillararene (a unique macrocyclic host)-mediated SDDS for the delivery of smart nanodrugs for siRNA, fluorescent molecules, and insulin for juvenile diabetes. Furthermore, fundamental questions and future hurdles related to smart SDDS based on CB[7] and pillararenes and their future promising breakthrough implementations are also distinctly outlined in this Review.

1. INTRODUCTION

Supramolecular chemistry, as elucidated by one of its eminent proponents, Jean Marie Lehn, as “chemistry beyond molecules”, has been identified as an incredible approach in biomedical applications having immense potential for diagnosis and therapeutic treatment with the reason rooted in their hydrophobic cavity and their controllable components.¹ Supramolecular nanodrug carriers are developed by several noncovalent interactions like hydrophobic interaction, electrostatic attraction, hydrogen bonding, π - π interactivity, etc. These nanodrug carriers have been placed in frontiers of recent research due to their acute potential for artificial modification and firm encapsulation. They have reasonable binding constants to reduce the tendency of guests to undergo unwanted aggregation, thus leading to diversification of drug delivery systems. The synergy between various organic guest molecules and the water-soluble macrocyclic

host molecules are prototype illustrations of supramolecular interactions.² Reversibility of host–guest complexation is an essential criterion for partial or complete retention of therapeutic activity of encapsulated drugs.^{1–9} Cucurbit[n]urils (CB[n], $n = 5–10$) are a novel category of barrel-shaped water-soluble cyclic oligomers, composed of “ n ” number of glycoluril units laced by two methylene groups (Figure 1).^{10–12} CB[n] is a rigid hydrophobic container having two symmetrical orifices composed of n carbonyl units, which

Received: July 27, 2023

Revised: November 10, 2023

Accepted: November 20, 2023

Published: December 4, 2023



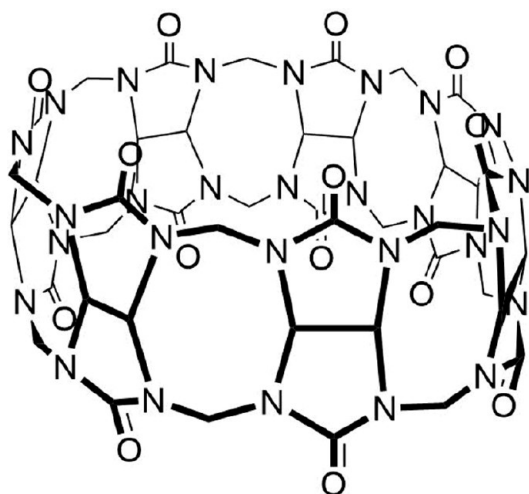


Figure 1. Illustration showing the chemical structure of cucurbit[7]uril (CB[7], 1).

assists it to bind molecules bearing positive charges or cations firmly. Interestingly, the neutral and the hydrophobic guest molecules can also be housed inside the nonpolarizable and hydrophobic CB[*n*] cavity.^{13,14} In fact, important drug molecules can mimic these incorporated guest molecules necessary for advanced drug delivery applications,^{15–17} or it can be an optically active fluorescent dye for sensing applications^{18–20} or a polymeric guest for scaffolding smart nanomaterials.^{21–23} Along this line of research, several other macrocyclic containers have also been developed and were drawn to the fields of interest like cyclodextrin,^{24–29} calixarene,^{30,31} metallostructures,^{32–34} etc. There are certain properties that make CB[*n*] stand out in particular, which are their low cellular toxicity,³⁷ high stabilization of incorporated drugs,^{4–7} high binding constant for cationic guests,^{35–38} effective shifting of the p*K*_a of encapsulated guests,^{36,39–41} and supramolecular catalysis of hydrolytic reaction.⁴²

Pillararenes (PA[*n*]), another emerging novel family of macrocyclic cavity bearing host molecules, were first synthesized and coined by Tomoki Ogoshi in 2008.⁴³ Their unique pillar-shaped structure and simplistic functionalization have received burgeoning attention because they endow them with distinct capabilities to selectively bind various kinds of important guests.⁴⁴ Pillararenes paved well their way toward application of nanomaterial,^{45–47} molecular recognition,^{48–51} chemosensors,^{52–54} ion transport,⁵⁵ supramolecular polymers,^{56,57} transmembrane channels,⁵⁸ light-harvesting systems,^{59,60} nonporous adaptive crystals,^{61,62} and hydrogels.⁶³ Water-soluble pillararenes not only exhibit excellent biocompatibility and low pH-sensitive properties in aqueous media but also show strong binding ability for different types of guest molecules. PA[*n*]'s hydrophobic cavities are quite adaptive (*n* = 5–10), fetching enough scope not only to augment the host–guest complexation but also to develop more types of supra-amphiphiles including head-to-tail tadpole-like, bola-type, gemini-type, macrocyclic, and polymeric amphiphiles. Higher-order aggregates like vesicles, micelles, or nanoparticles can be achieved for controllable anticancer drug delivery⁶⁴ by tuning pillararene-based amphiphilic supramolecular host–guest complexes in such a way that they can even further self-assemble to form the desired drug-loading vehicle. In the line with the fascinating

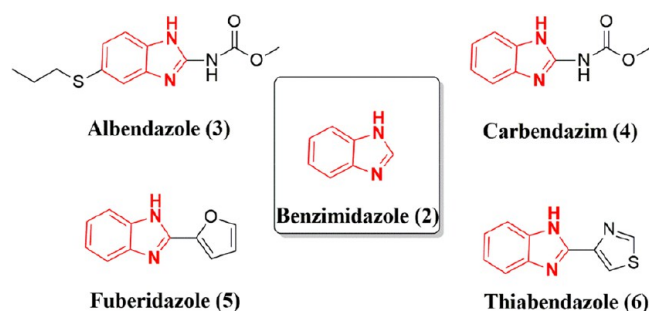
research on host–guest properties, it is highly well-timed to develop stimuli-responsive polymersomes self-assembled from PA[*n*]-based supramolecular block copolymers as targeting SDDS for effective anticancer therapy.⁶⁵ Pillararene-based supramolecular nanocarriers for effective chemo-photodynamic dual therapy are also examined in this Review.

2. CUCURBIT[7]URIL (CB[7], 1)

2.1. SDDS Formed by CB[7]-Encapsulating Benzimidazole-Derived Drugs.

In recent research studies, it has been revealed that benzimidazole (BZ, 2) residue has a great affinity for CB[7].^{9,66,67} Photophysical properties, photochemical stabilities, and aqueous solubilities of several BZ residues like albendazole (ABZ, 3), carbendazim (CBZ, 4), fuberidazole (FBZ, 5), thiabendazole (TBZ, 6) (Scheme 1),

Scheme 1. Chemical Structures of the Benzimidazole Molecule and Its Derivatives



and their mother compound benzimidazole (BZ) with CB[7] are thoroughly investigated using UV–vis and NMR spectroscopy techniques, which reveal that CB[7] binds and stabilizes the protonated form of the above-mentioned anthelmintic drugs of the BZ family in water very robustly (e.g., $K = 2.6 \times 10^7 \text{ mol}^{-1} \text{ L}$ for ABZ) but encapsulates their unprotonated forms very feebly (e.g., $K = 6.5 \times 10^4 \text{ mol}^{-1} \text{ L}$ for ABZ),⁶⁸ which signifies increase in p*K*_a value upon complexation with CB[7]. In water ABZ, TBZ, CBZ, FBZ, and BZ showed far UV absorption of <320 nm and fluorescence in the region of 290–360 nm at pH 7.2, but at lower pH values, the absorption spectra undergo slight but distinct shift due to protonation of the benzimidazole residue. The change in the optical density (OD) at the peak maximum of the absorption spectra of BZ residues like ABZ, TBZ, CBZ, and FBZ is observed in the absence and presence of CB[7] at various pH values (Figure 2). UV titration was done to determine the host–guest binding constant (Table 1). CB[7], being a cation receptor, shows a consistently more significant binding constant with the protonated guest molecules than the neutral forms (ca. 2 orders of magnitude larger).

To investigate the structural features of these host–guest-complexed drug molecules, ¹H NMR study was performed only to realize that during the complexation of FBZ in D₂O at pH 2 the imidazolium protons are upfield shifted when complexed with CB[7] of up to 1 ppm. In contrast, the furanyl protons are either barely affected or even undergo downfield shift (Figure 3).

The same observations are reported for other BZ residues also, which reflects preferential inclusion of the imidazolium moiety of BZ residue inside the CB[7] cavity while the furanyl ring is protruded out near the rim. Similarly, for ABZ,

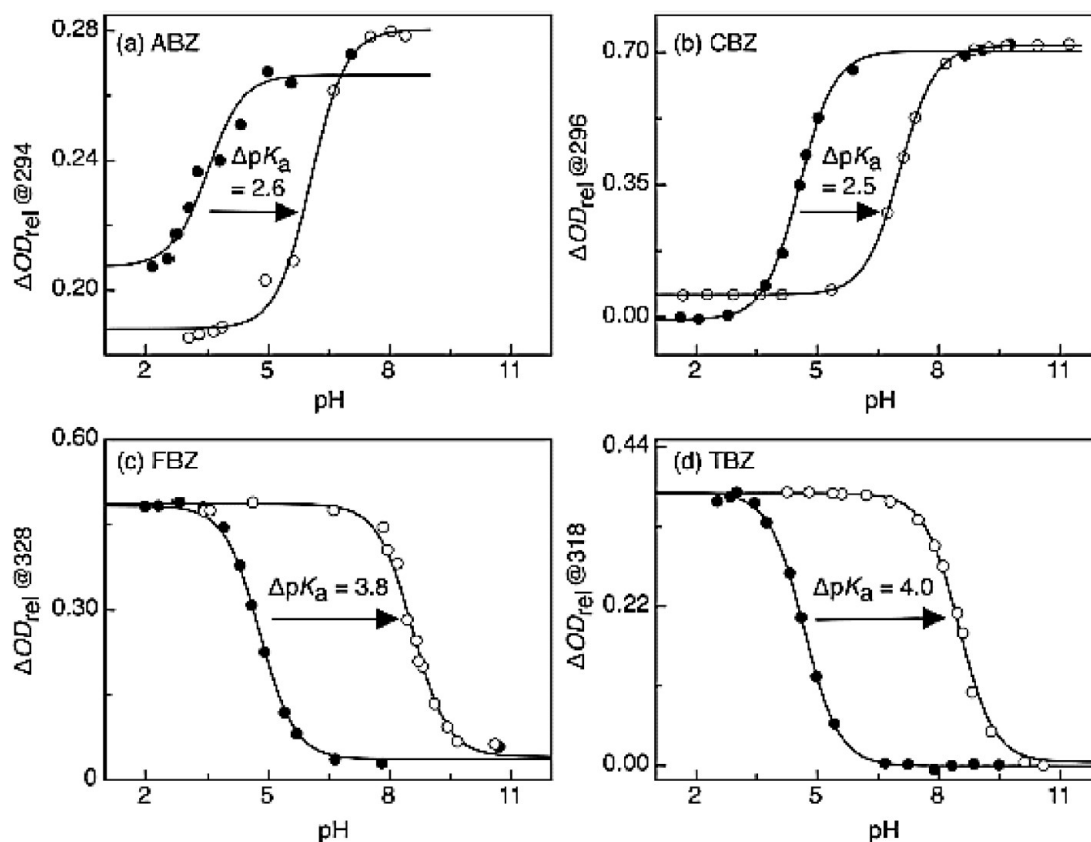


Figure 2. pH titration plots of the BZ drugs, tracked by UV in the absence (filled circles) and presence of CB[7] (2.5 mmol L⁻¹, empty circles).⁶⁸ Reprinted with permission from ref 68. Copyright 2022, Canadian Science Publishing.

Table 1. pK_a Values of Uncomplexed (pK_a) and the CB[7]-Complexed Form (pK_a') of BZ Derivatives in Water^{68,a}

guest	pK _a	pK _a '	ΔpK _a	K _{BZ} (10 ³ mol ⁻¹ L)	K _{BZH⁺} (10 ³ mol ⁻¹ L)
ABZ	3.5	6.1	2.6	65	26
CBZ	4.5	7.0	2.5	24	76
TBZ	4.6	8.6	4.0	0.150 ± 0.025	1.5
FBZ	4.8	8.6	3.8	0.05 ± 0.01	0.32
BZ	5.5	9.0	3.5	1.5	4.7

^aReproduced with permission from ref 68. Copyright 2011, Canadian Science Publishing.

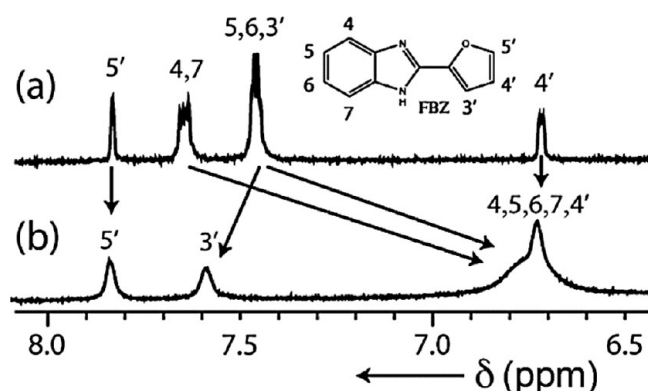


Figure 3. ¹H NMR-based spectral plot of 0.25 mmol L⁻¹ FBZ (a) in the absence of CB[7] and (b) in the presence of 2.5 mmol L⁻¹ CB[7] in D₂O at pD 2.4.⁶⁸ Reprinted with permission from ref 68. Copyright 2011, Canadian Science Publishing.

the hydrophobic propylthio moiety is the only one adequately encapsulated inside the CB[7] macrocycle, proved

by its upfield shifts. To further delve into this observation, a negative control experiment was conducted in which a smaller macrocycle, CB[6], was taken instead of CB[7], which showed that it could not encapsulate the BZ ring due to its smaller cavity but can only encapsulate the other smaller groups of the BZ residues like carbamate methyl groups of ABZ and CBZ (upfield shift of 1 ppm). The carbonyl portal of CB[7] gives an additional stabilization of the protonated form of these guest molecules by dint of the ion–dipole interaction. The guest molecule is easily protonated when it is complexed with CB[7], which is reflected in the experimental data of larger pK_a shift in the case of complex formation with CB[7]. Though these benzimidazole-derived drugs are extensively used as fungicide and anthelmintic drugs,^{33,69–74} their only common drawback is their poor aqueous solubility, which is very unacceptable as a feature of anthelmintic drugs. So, to overcome this drawback, CB[7], a potential additive, is used for the solubility enhancement. Interestingly, by adding only 2 mmol L⁻¹ of CB[7], the solubility of ABZ, CBZ, TBZ, and FBZ can be enhanced by a factor of 100, 7, 10, and 3,

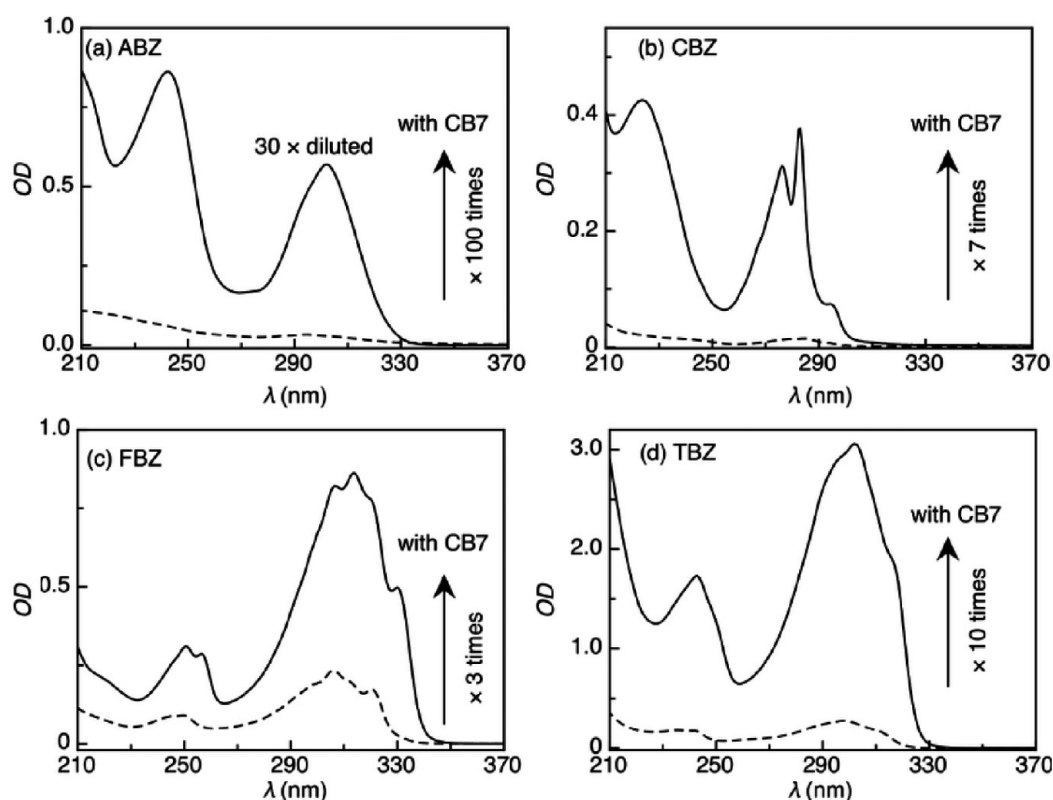


Figure 4. At pH 7.2, absorption spectra measured for the BZ drugs in the absence (dashed lines) and presence of CB[7] (2.0 mmol L^{-1} , solid lines). The arrows show the enhancement of the solubility factors. Note that the solution taken for UV spectroscopic analysis is 30 times diluted in order to obtain an OD value inside the instrumental range.⁶⁸ Reprinted with permission from ref 68. Copyright 2011, Canadian Science Publishing.

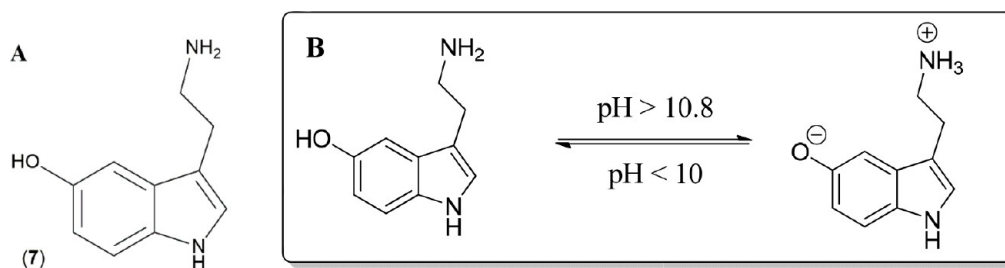


Figure 5. (A) Diagram showing chemical structure of serotonin (SRT, 7) (B) Prototropic equilibrium of SRT with different pH values.

respectively (Figure 4). Thus, the CB[7] macrocycle acts as a promising candidate for drug solubilization of these types of least soluble drugs. The photostability of TBZ and FBZ is enhanced by CB[7] encapsulation, with the result that FBZ decays 7 times slower and TBZ 3 times slower when complexed by CB[7] than their free states. For the rest of the drug molecules, the photostability effect is not so significant.

These types of prospective applications of cucurbituril are also exhibited by β -cyclodextrin but of lower efficiency because a very high concentration of β -cyclodextrin is required to compete with that of cucurbituril. This can be due to the lower binding constant of β -cyclodextrin and its inability to induce protonation. Thus, cucurbituril wins the spotlight of being the most unique and novel futuristic drug carrier.

2.2. SDDS Formed by CB[7]-Encapsulating Neurotransmitter Hormone Serotonin (7). Serotonin (7) or 5-hydroxytryptamine (Figure 5a) is a naturally occurring monoamine neurotransmitter for the central and peripheral

nervous system. It is a multifaceted key hormone responsible for mood modulation like sleep, addiction, cognition, learning, memory, aggression, food intake, nausea, and anxiety widely formed in the brain by the serotonergic neurons. Serotonin (SRT, 7) was first discovered by Vittorio Erspamer, an Italian pharmacologist, in 1952,⁷⁵ and later Walther et al. synthesized it by a second tryptophan hydroxylase isoform in 2003.⁷⁶ Sudden imbalance of the serotonin level in the body can cause serious mental disorders like Alzheimer's disease, schizophrenia, infantile autism, and depression as stated by Dubovsky and Thomas in 1995 and Voet and Voet in 2006.⁷⁷ SRT was reported to exhibit different fluorescence properties by Kishi et al. in 1977.⁷⁸ SRT has primarily two pK_a values, one at 9.97 for an aliphatic amino group and one at 10.73 for an aromatic hydroxyl group (Figure 5B). Considering the acute diseases caused by the disorder of the SRT level in our body, the delivery of SRT is essential through the supramolecular drug delivery system for effective therapy against various SRT syndromes.

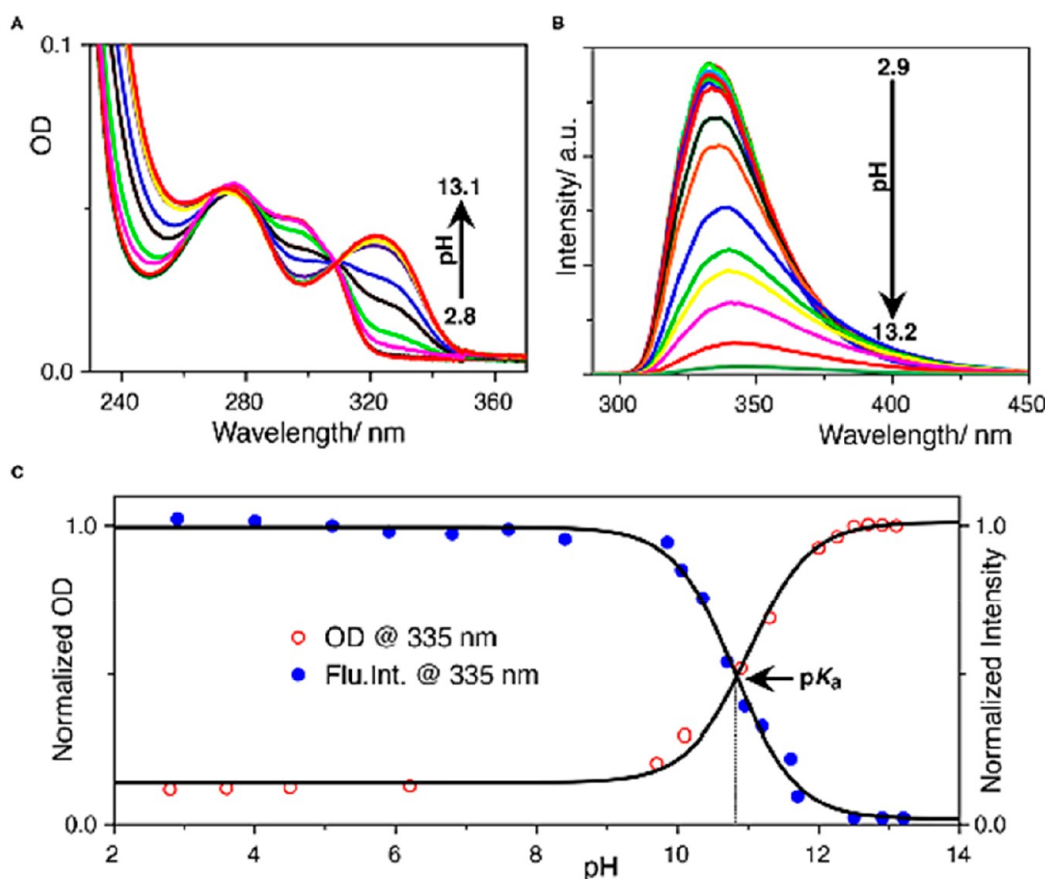


Figure 6. (A) UV–vis-based pH titration graph showing the surge of the 333 nm absorption peak with increasing pH, (B) fluorescence-based pH titration graph illustrating the quenching of the fluorescence peak at 335 nm with pH, and (C) determination of the pK_a value from UV–vis and fluorescence titration. The normalized optical density at 333 nm and the fluorescence intensity at 335 nm are plotted against the pH of the solution.⁷⁹ Reprinted from ref 79. Copyright 2020, Frontiers.

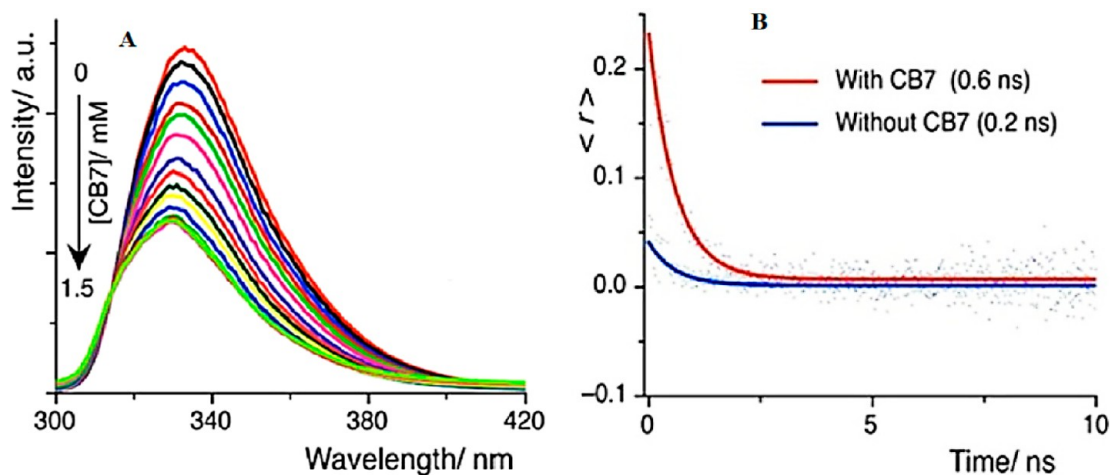


Figure 7. (A) Fluorescence titration of SRT with CB[7] at pH 3.0; encapsulation leading to a gradual decrease of the intensity peak, and (B) time-resolved anisotropy decay plot of SRT in the presence and absence of CB[7] at pH 3.⁷⁹ Reprinted from ref 79. Copyright 2020, Frontiers.

Thus, for the encapsulation of such a hydrophobic guest molecule, a rigid and hydrophobic macrocyclic molecule is required, and CB[n] was chosen for this vehicular purpose. This is so because the encapsulation led to a significant shift in pK_a value, enhancement of the solubility factor of the drug molecule, sustained release of drug, and sensing via electronic spectroscopy for an optically active molecule.⁷⁹ Upon CB[7] encapsulation SRT exhibited pH-dependent binding affinity.

The photolytic activity of SRT is very much pH sensitive to the surrounding solution. In low pH, two absorption maxima, one at 277 nm and another at 297 nm, are exhibited by SRT, while at basic pH, the 297 nm band gets quenched and the band with maximum at 325 nm gets developed (Figure 6), leading to a bathochromic shift due to an increase in the resonance of the chromophoric unit. This phenomenon happens due to the deprotonated phenolic –OH group

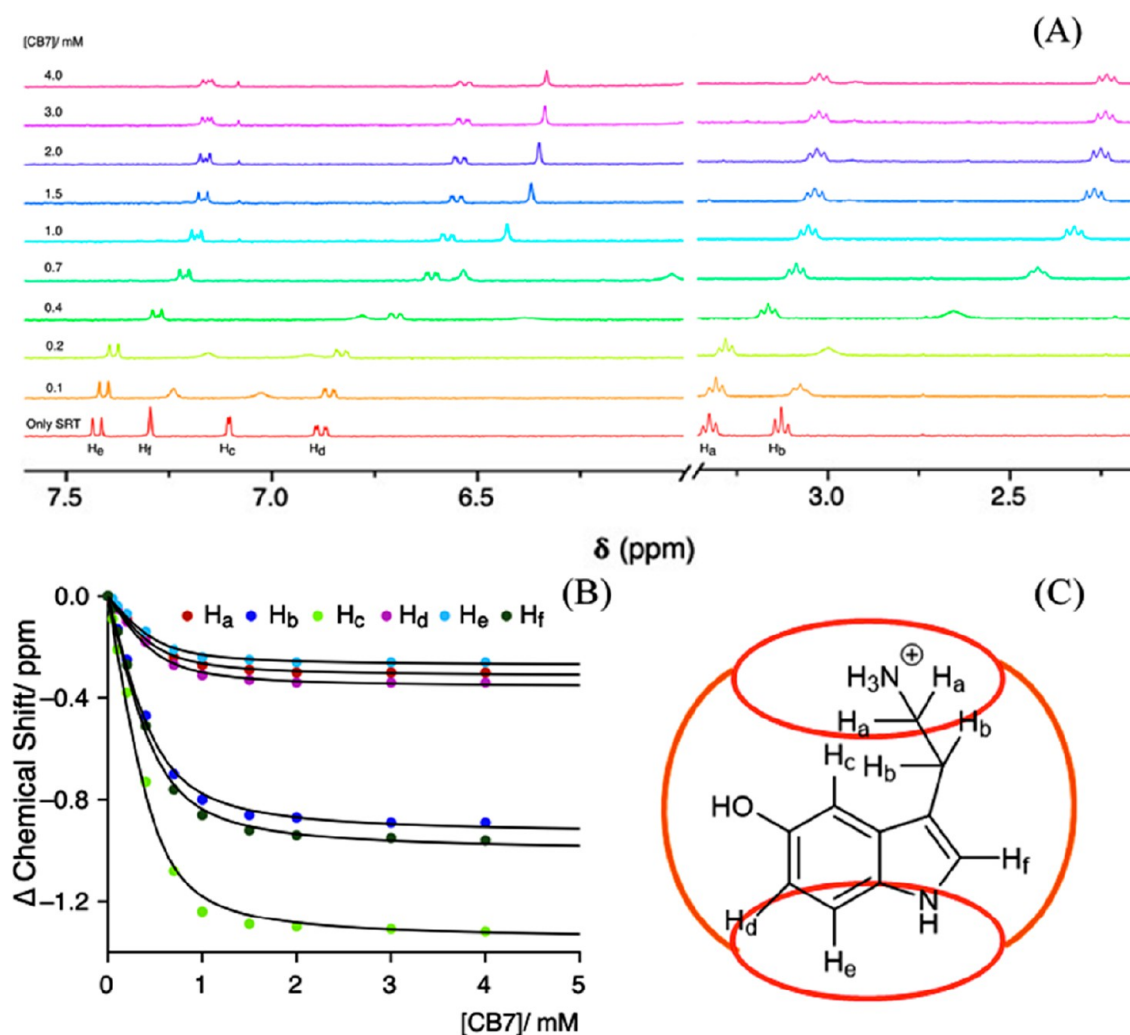


Figure 8. (A) NMR titration plot of 0.5 mM SRT with increasing concentration of CB[7] up to 4.0 mM at pD 2.8; the aromatic region and the aliphatic region are illustrated in the left zone and the right zone of the NMR titration plot, respectively, (B) fitted plot of the variation in complexation-induced shift (CIS) against the concentration of CB[7], and (C) pictorial representation of the feasible SRTH⁺-CB[7] complex.⁷⁹ Reprinted from ref 79. Copyright 2020, Frontiers.

of the indole ring, and as a result, the phenolate ion undergoes ring resonance. The transition between the unprotonated and the protonated form is aptly denoted by the isosbestic point at 309 nm. Upon exciting at 280 nm at different pH values by fluorescence spectroscopy, it was observed that the intensity tends to be negligible with increasing pH. This observation can be explained by the poor absorbance value of the ionized species at the excitation wavelength, which is followed by the continuous weakening of the intensity above the physiological pH. The reported acid dissociation constant of the primary amine of SRT is 9.9. The pK_a values gathered from the pH titration using absorption and emission spectroscopy are the same. This signifies that no alteration is observed in the pK_a value upon electronic excitation. UV-vis titration of 5 μM SRT at pH 3.0 with a gradual increment in the concentration of the CB[7] resulted in an isosbestic point at 280 nm reflecting the perfect encapsulation of SRT in the CB[7] macrocycle. To get additional evidence of encapsulation, fluorescence titration was performed again with increasing concentration of CB[7] along with 10 μM SRT at pH 3.

Upon increasing the amount of CB[7], the fluorescence intensity progressively gets quenched, and saturation was only obtained after the incorporation of 1.5 mM CB[7] (Figure 7A). Thus, the attenuation of fluorescence intensity signifies a strong host-guest encapsulation. To determine the rotational restriction experienced by the SRT molecule in the macrocyclic cavity of the CB[7], time-resolved anisotropy decay measurement was done at acidic pH (pH ~ 3.0), which fetched the result that the anisotropy of SRT got a surge from 0.2 to 0.6 ns upon treatment with CB[7] (Figure 7B). The higher anisotropy value of SRT in the presence of CB[7] at acidic pH signifies the restriction of free rotation posed by the hydrophobic cavity of CB[7].

At higher pH, no change in anisotropy is observed due to feeble complexation. To find out the complexation-induced shift (CIS), NMR study was performed. At acidic pH (pD 3.0), an intense upfield CIS was observed for H_b, H_c, and H_f, which bears evidence that those hydrogen atoms of SRT are rooted inside the cavity of the CB[7] (Figure 8). Conversely, a small upfield CIS for H_a, H_d, and H_e signifies that these protons are present relatively nearby to the rim of the CB[7]. With the intention to check the stability and the depth of the

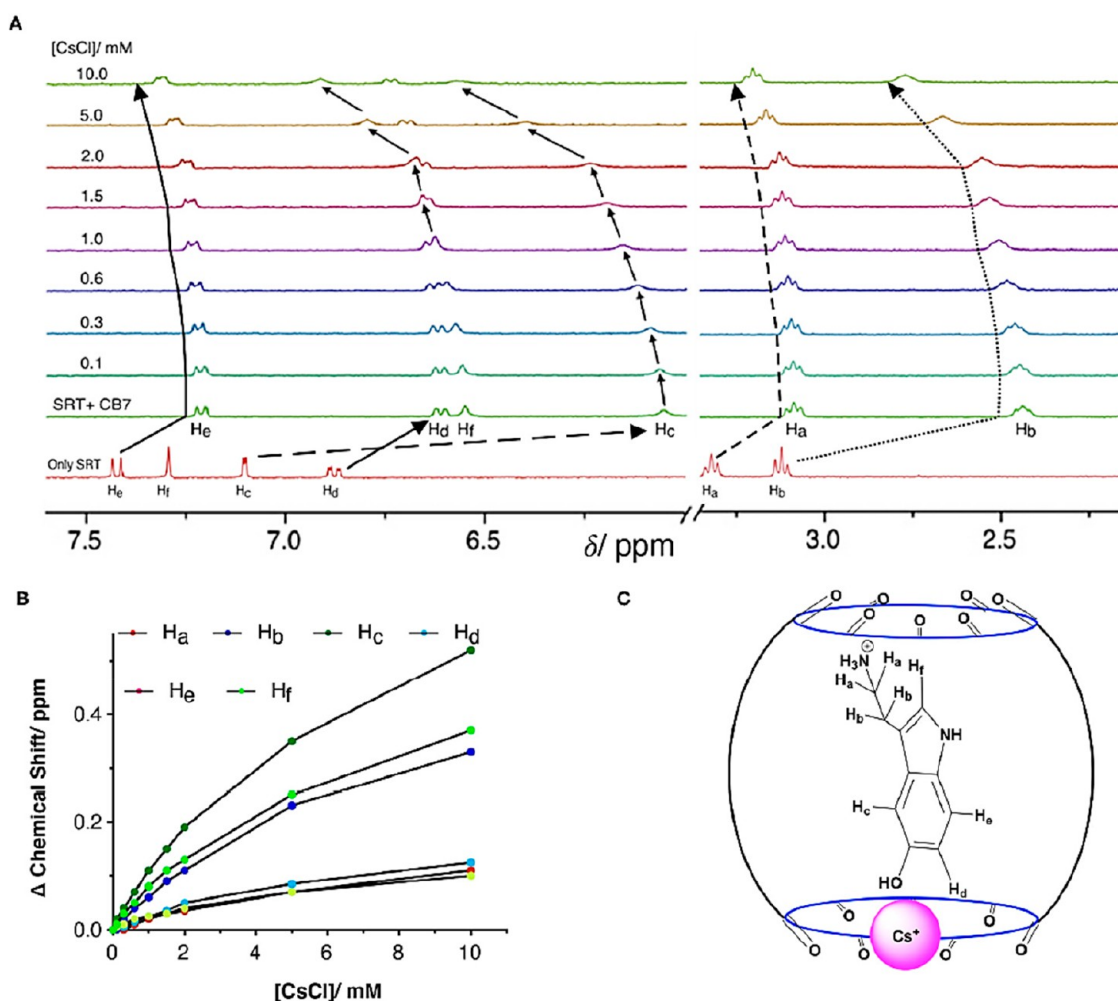


Figure 9. (A) NMR titration plot of the SRT-CB[7] (0.5 mM SRT) complex with increasing concentration of CsCl up to 10 mM at pH 2.5; left portion shows the aromatic region and the right portion shows the aliphatic region of the NMR spectra. (B) A fitted plot illustrating the difference in chemical shift values (in ppm) against the concentration of CsCl. (C) Diagrammatic illustration of the SRT-CB[7]·Cs⁺ complex.⁷⁹ Reprinted from ref 79. Copyright 2020, Frontiers.

inclusion complex SRT·CB[7], competition titration was done with cesium. At first, Cs⁺ binds to the mouth of CB[7], and then, by reorienting SRT, it forms a ternary complex SRT·CB[7]·Cs⁺ (Figure 9) where Cs⁺ forms a lid to one side of CB[7], which was further validated by fluorescence titration. Thus, the path for SRT delivery is promisingly paved by CB[7], considering it to be a very significant neurotransmitter.

2.3. Encapsulation of Norharmane Drug (8) by CB[7]. Norharmane (NHM, 8), a β -carboline-based drug, is a nitrogen-containing heterocycle that commonly acts as a GABA (gamma-aminobutyric acid) agonist (Figure 10). It is an active alkaloid which has an anxiogenic and memory-enhancing effect. It is composed of a π -electron-rich indole

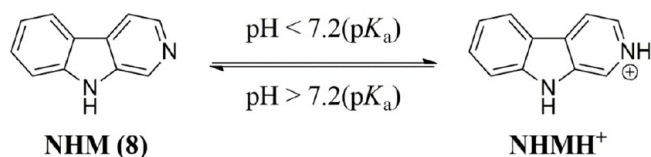


Figure 10. Structure of norharmane (NHM, 8) and the protolytic equilibrium between its neutral and protonated forms (NHMH⁺).

ring and a π -electron-deficient pyridine ring.^{80,81} Pharmacologically, it is a type of hallucinogen which has antitumor activity. It is also produced endogenously from the human body⁸² as well as being a photoproduct from tryptophan in the human eye lens.^{80–82} Recently, it has been used as photosensitizers for virus, bacteria, and fungi with a remarkable DNA binding constant,^{83,84} but like other drugs mentioned above, it also faces the same drawback of poor water solubility. Its solubility can be enhanced if it is provided with an amphipolar and microheterogeneous cavity. The micellar environment provided by the well-organized assemblies of surface-active agents or macrocyclic containers does have a massive impact on the bioavailability,⁸⁵ photophysical, and chemical properties of these β -carboline-based sparingly water-soluble drugs. The hydrophobic nanocavity of the caged macrocycles, just like biological organization, encapsulates drug molecules with high binding affinity.⁸⁶ In the last few decades, CB[n] and acyclic type CB have been used extensively as a drug delivery vehicle for sparingly water-soluble drugs.^{35,66,68,87,88} The factors by which incorporation of CB[7] can enhance the solubility of the sparingly soluble drugs at neutral pH have been compiled in Table 2.

Table 2. Solubility Improvement Factor of Poorly Soluble Drugs Using CB[7] at Neutral pH^{89,4}

drugs category	drug	solubility enhancement with CB[7] (pH 7.0)
anthelmintic drugs	benzimidazole	2
	fuberidazole	3
	carbendazim	7
photosensitizer	norharmane	12
	testosterone	5
	progesterone	21
anticancer drug	camptothecin	70
	gefitinib	102
antileprosy	clofazimine	63

⁴Reproduced with permission from Ref 89. Copyright 2018, Elsevier.

As the stability of the self-aggregated micelles depends upon factors like pH, temperature, viscosity, and ionic strength, it is not suited for drug delivery applications. At near-neutral pH value of NHM, the CB[7] nanocavity can modulate its optical properties. To estimate the binding interaction of NHM with CB[7], fluorescence binding titration was performed using 6 μ M NHM with increasing concentration of CB[7] macrocycle at pH 3. The 450 nm band (Figure 11) was seen to be attenuated along with a 5 nm hypsochromic shift. This phenomenon strongly relates hard-core binding of NHMH⁺ with CB[7] at acidic pH.

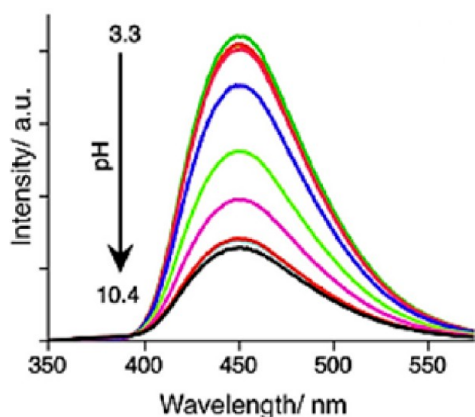


Figure 11. Excited-state pH titration plot of NHM.⁸⁹ Reprinted with permission from ref 89. Copyright 2018, Elsevier.

NHMH⁺ experiences preferential stabilization in CB[7] over neutral ones, which is evident from the similar titration performed with neutral NHM that showed less average lifetime of NHM than NHMH⁺ in CB[7]. For further exploration of the effect of encapsulation phenomena on excited-state lifetime and anisotropy decay of NHM in different types of microenvironments, time-resolved fluorescence spectroscopy was performed, which showed that at acidic pH, NHMH⁺ had a fluorescence lifetime of only 22.0 ns when decay was at 450 nm. The fluorescence decay graph is a biexponential decay type along with a longer lifespan and shorter component. The two different lifetime components in the fluorescence decay signify that both the neutral and the protonated species are in equilibrium. For investigation of solubility enhancement of the drug molecule by CB[7], UV–vis spectroscopy is conducted only to find that the solubility of NHM is enhanced by a factor of 14.0, 12.0, and 9.0 at low (pH 3.0), physiological (pH \sim 7.0), and high pH (pH 12.1), respectively, upon the incorporation of 4.0 mM CB[7]

(Figure 12). Such solubility enhancement is a much-needed requirement for the poorly soluble β -carboline-based drugs. The NHM-CB[7] complex showed an increased cellular uptake compared to that of the free species when both were incubated with MCF-7 cells, evident from the high-intensity fluorescence from NHM entering the nucleus via CB[7]. Thus, CB[7] showed a ray of light for the NHM drug to be used on a wider scale without looking at any major hindrances or restrictions related to its delivery process inside our biological system.

2.4. Activation and Stabilization of Proton Pump Inhibitor Drugs by Cucurbituril. Encapsulation of drugs by CB[7] manifests a shift in the excited-state protonation equilibrium.⁹⁰ Pluth et al. recently demonstrated an interesting example of pK_a shift with the metal–organic supramolecular host having values extending up to 4.5.⁹¹ Proton pump inhibitor drugs are a category of medications which are used for reducing prolonged stomach acid production which can lead to gastroesophageal reflux along with duodenal ulcers. They inhibit the stomach's H⁺/K⁺ ATPase irreversibly. Lansoprazole (9a) and omeprazole (9b) (Scheme 2) are two examples of proton inhibitor drugs administered orally. The major drawbacks of these types of drugs are (i) prolonged conversion into cyclic sulfenamide (9c) as this active species can only react with the cysteine residues of the stomach's H⁺/K⁺ ATPase and (ii) rapid dimerization and decay of the active state in a very short time when exposed to highly acidic pH of the stomach.

So, to overcome these drawbacks the addition of CB[7] can be a way out as it helps in activation and stabilization. CB[7] not only catalyzes the formation of the active form of the drug (9c) but also enhances the stability of the cyclic sulfenamide (9c). UV spectroscopy is done to follow the kinetics of activation and disintegration of the drug (Figure 13). The UV absorption maxima at 340 nm (Figure 13 inset) signifies the active form. An increase in rate was observed from 0.2 to 3 min⁻¹ which reveals that the half-life period of formation was reduced from 5 min to 20 s upon the addition of CB[7] (0.05–5 mM). Upon adding CB[7] (5 mM), the half-life of the active species increased from 60 min to more than 3 weeks at pH 2.9. Moreover, in the presence of CB[7] the reactive intermediate exhibits a nice and clean ¹H NMR spectrum in D₂O (Figure 14). Omeprazole also exhibited a similar type of favorable effect upon encapsulation by CB[7]. To validate the inclusion of a proton pump inhibitor with CB[7], a competitive experiment was done with cadaverine (pentane-1,5-diamine). Cadaverine forms a strong inclusion complex with CB[7], thus dislodging the omeprazole from the cavity into free solution where it undergoes rapid

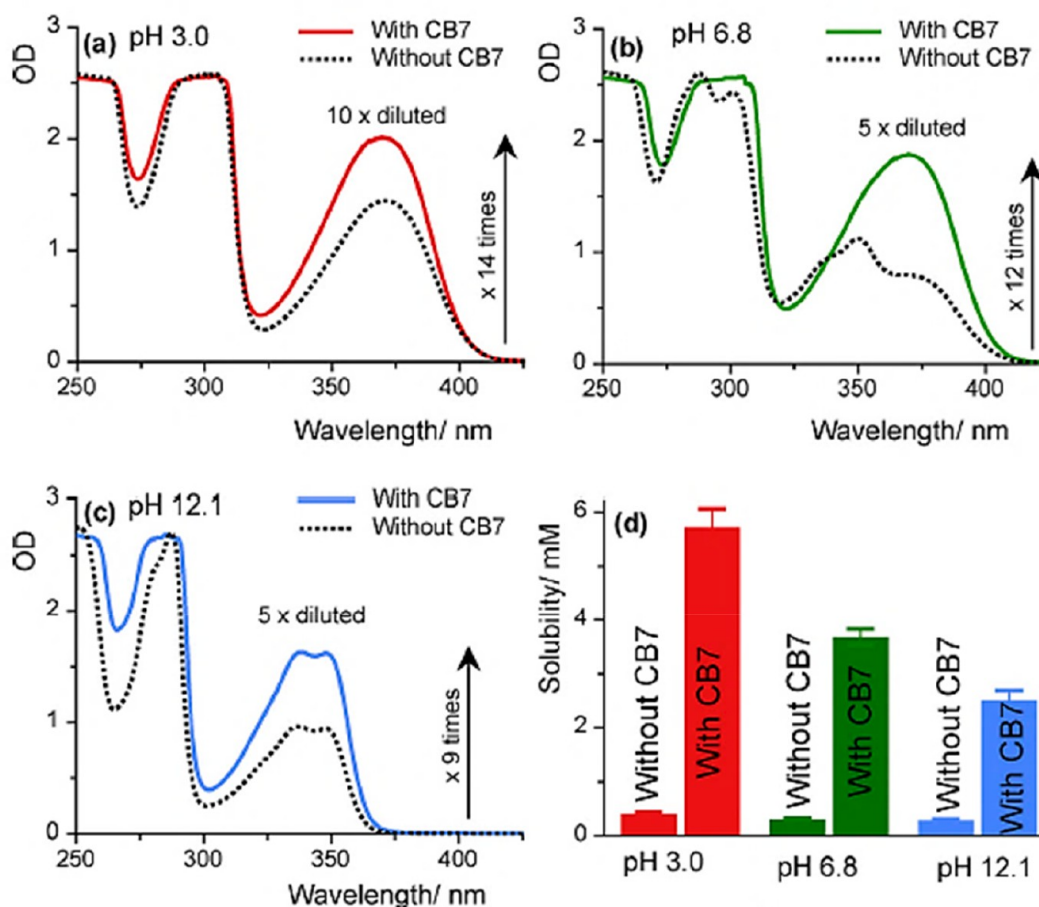
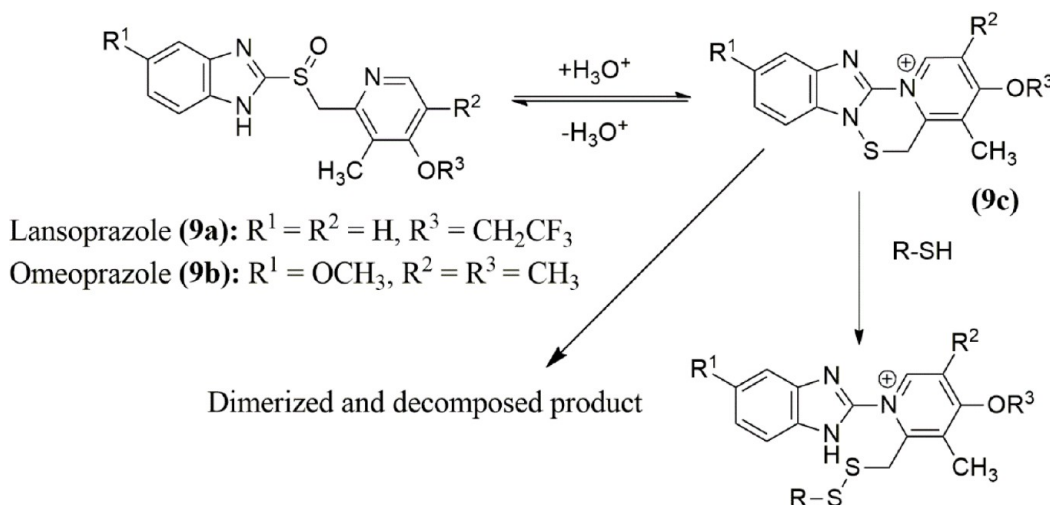


Figure 12. Absorption spectra plot of free NHM in the absence of CB[7] (dashed lines) and the presence of 4.0 mM CB[7] (solid line) at (a) pH 3.0, (b) pH 6.8, and (c) pH 12.1. (d) Bar-diagram illustrating the following solubility enhancement factor with CB[7]. The error bar shows the standard deviation from triplicated measurements.⁸⁹ Reprinted with permission from ref 89. Copyright 2018, Elsevier.

Scheme 2. Lansoprazole (9a) and Omeprazole (9b)



decomposition (half-life 60 min). However, unfortunately, direct determination of the binding constant and the pK_a shift was not possible due to the lability of both free species in aqueous solution. CB[7] helps in tuning of protonation equilibrium, thus aiding in rapid activation, but this strategy is somewhat unconventional because during supramolecular pK_a shift, along with increasing the basicity of the

benzimidazole group, it also affects the nucleophilicity and the basicity of the pyridine moiety on a smaller scale.

2.5. Encapsulation of a Platinum Anticancer Drug by CB[7]. Among several platinum anticancer drug complexes, cisplatin (10a) (Figure 15a) is a highly competent drug for the treatment of human neck, head, bladder, lungs, testicular, as well as ovarian cancer.⁹² Despite its high

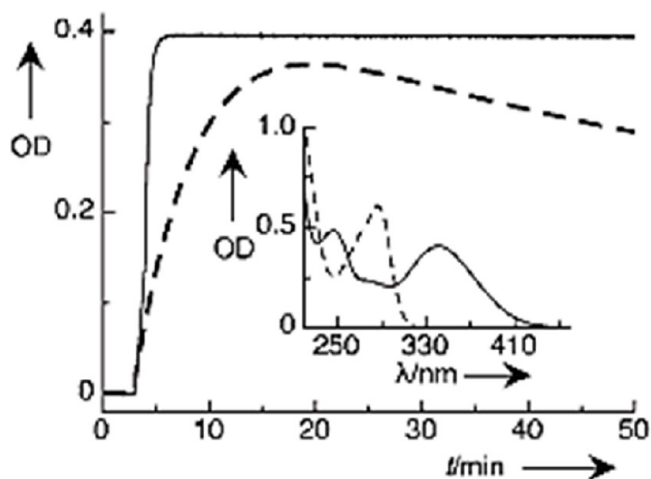


Figure 13. Upon dissolving **9a** (50 mM) in aqueous solution at pH 2.9, the active form evolved followed by UV spectroscopy ($\lambda_{\max} = 340$ nm) in the absence (dashed line) and presence (solid) of 0.2 mM CB[7]. The inset plot shows the UV spectra of **9a** (dashed line, straightaway after dissolution in the absence of CB[7], $\lambda_{\max} = 287$ nm) and of the complex **9a**:CB[7] (solid line, with 1 mM CB[7] after 3 min, $\lambda_{\max} = 340$ nm).⁶⁶ Reprinted with permission from ref 66. Copyright 2008, Wiley-VCH.

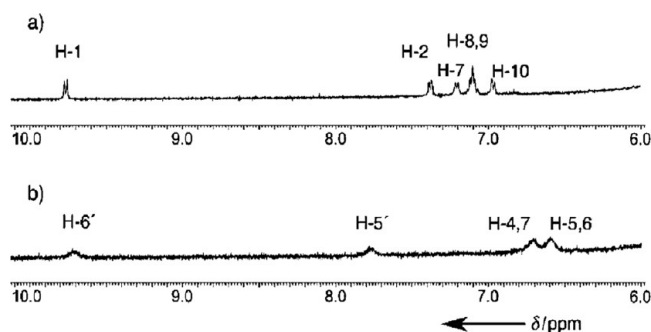


Figure 14. ¹H NMR-based spectra of the aromatic region recorded in D₂O of (a) the **9a**:CB[7] complex (2 mM **1a**, 5 mM CB[7]) at pD 3.3 and (b) the disulfide adduct **3a** obtained in situ from the **9a**:CB[7] complex (0.75 mM **1a**, 3 mM CB[7]) upon adding 2.0 mM cysteine.⁶⁶ Reprinted with permission from ref 66. Copyright 2008, Wiley-VCH.

effectiveness in cancer treatment, its prolonged use can be hindered by some of its acquired and innate restrictions.⁹³ Such factors are low cellular uptake, deactivation of the drug by increase in the body's glutathione level, or increase of the tolerance level of DNA lesions against such platinum-based drugs.⁹⁴ Moreover, cisplatin is also accompanied by several side effects like nausea and nephro- and neurotoxicity which has certainly limited its dose level between 60 and 120 mg m⁻².⁹⁵ Due to such complexities, several other platinum-based drugs are approved like carboplatin and oxaliplatin, and many multinuclear platinum complexes are also simultaneously being developed. Multinuclear platinum-based complexes are expected to overcome the limitations through novel DNA-binding linkages. Unlike cisplatin and carboplatin, the multinuclear complexes generally form pliable and long-range interstrand adducts which can be easily taken up by the biological cells more than cisplatin. BBR3464 (**10b**) (Figure 15b) is among one such complex which has potentially made its entry in phase II clinical trials, and BBR3571, BBR3610, and BBR3611 have also showed immense capability in this field.^{94,96–99}

Though these complexes require very low concentration for their activation compared to cisplatin, their toxicity levels are very high. Moreover, these complexes can be deactivated by the body's plasma proteins before reaching their targets thus showing low activity. Thus, to curb their toxicity and easy degradation, cucurbiturils can be chosen as an effective host for the delivery of platinum-based multinuclear complexes. The complexation of *trans*-[PtCl(NH₃)₂μ-dpzm]²⁺ (dpzm = 4,4'-dipyrazolylmethane) with CB[7] reduces the rate of reaction of platinum complex with guanosine without changing its usual DNA-binding mode.¹⁰⁰ In the case of complexation of oxaliplatin with CB[7], its reactivity is reduced for both guanosine and methionine along with the lowering of in vitro cytotoxicity. NMR study was done in each case of complexation of CB[7] with cisplatin, di-Pt (**10c**), and tri-Pt (**10d**) (Figure 15c and 15d).¹⁰¹ The study of the interaction between cisplatin and CB[7] was done by ¹H and ¹⁹⁵Pt NMR.¹⁰¹ Upon adding cisplatin, the CB[7]-CH resonance at 5.58 ppm bifurcates into two peaks, 5.63 and 5.55 ppm (Figure 16a and 16b).¹⁰¹ One peak is upfield shifted and is characterized by significant line broadening, while the other peak is comparatively sharp and downfield shifted.¹⁰¹

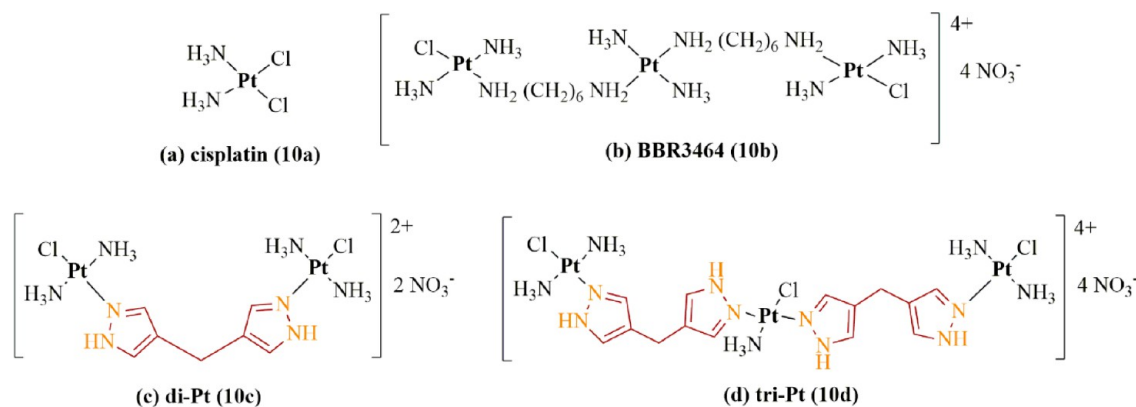


Figure 15. Structures elucidating cisplatin (a), a common multinuclear platinum-based complex conjoined with a ligand, BBR3464 (b), di-Pt (c), and tri-Pt (d).

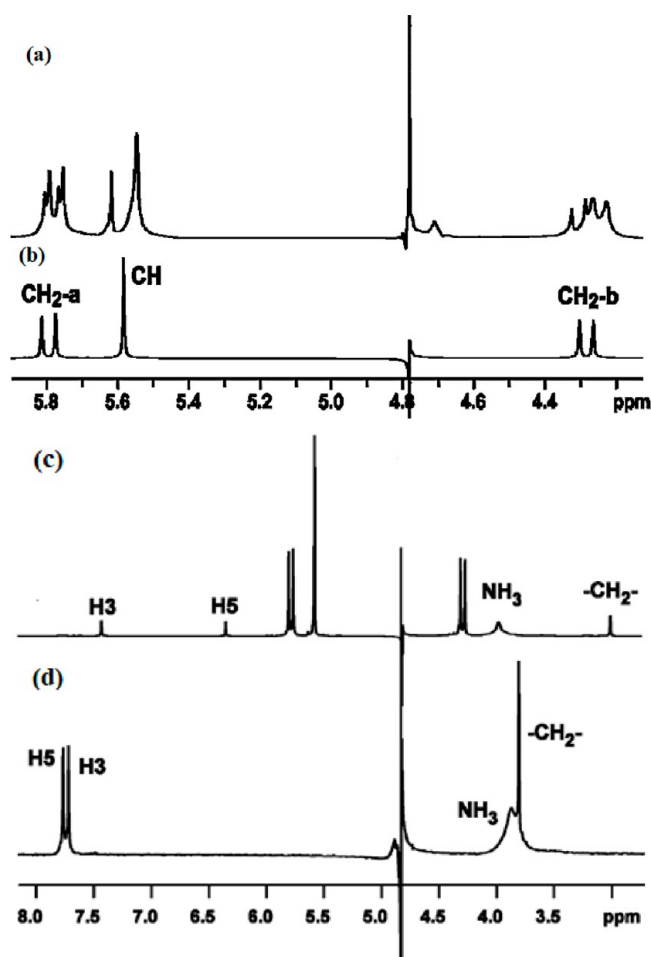


Figure 16. ^1H NMR spectra elucidating (a) CB[7] added with cisplatin at $R = 1$ at $25\text{ }^\circ\text{C}$ in D_2O solvent, (b) CB[7], (c) di-Pt, and (d) di-Pt encapsulated with CB[7] at $R = 1$.¹⁰¹ Reprinted with permission from ref 101. Copyright 2006. The Royal Society of Chemistry.

A similar characteristic is also observed for the peaks of the nonequivalent CB[7]-CH₂ protons. When the platinum complex is dissolved in slightly acidic water, an equilibrium is established between the chloro- and hydrated-forms of cisplatin, with the peak of Pt for *cis*-[PtCl₂(NH₃)₂] and *cis*-[PtCl(NH₃)₂(H₂O)]⁺ at -2160 and -1854 ppm, respectively.¹⁰¹ When CB[7] was added, the chloro form exhibited a second resonance at -2109 ppm, while the peak for the aqua form was majorly shifted to -1890 ppm.¹⁰¹ Separate peaks for uncomplexed and complexed chloro forms signify reduced exchange kinetics, thereby revealing that a part of the chloro form gets firmly encapsulated inside the CB[7] cavity. A large upfield shift of the dpzm resonances was observed when di-Pt was encapsulated in CB[8], with the di-Pt H₃ and methylene peak shifting to the same extent as that for CB[7] encapsulation.¹⁰¹ The H5 peak shifted upfield by only 0.94 ppm more than that in the case of CB[7] complexation (Figure 16c and 16d) which shows that the platinum-based complex is placed slightly differently in CB[8] than in CB[7].¹⁰¹ Moreover, the resonance due to the ammine protons of di-Pt shifted downfield with CB[7] encapsulation and shifted upfield upon CB[8] encapsulation which reveals that the $-\text{NH}$ protons are situated deep inside the cavity of CB[8], unlike CB[7]. The dpzm peak of the CB[8]

complexed with di-Pt is broader than that for CB[7] encapsulation which suggests that the transition rate between the CB[8] complexed di-Pt and the uncomplexed one is more rapid than for CB[7] encapsulation.¹⁰¹ This inference suggests that the rate of release and the toxicity of the Pt-based multinuclear drug can be tuned by the cavity size of CB[*n*] itself. From the ^1H NMR study, it is observed that the hydrolyzed di-Pt requires more time (ca. 24 h) to be encapsulated by CB[7] than the unhydrolyzed one which is evident from the large upfield shift in the dpzm resonance of the aqua di-Pt complex.¹⁰¹ This same inference can also be derived for the tri-Pt complex as a very high energy is required for the +2-platinum center to get into the CB[*n*] portal. The encapsulation of tri-Pt is slightly different for CB[7] and CB[8] with distinguishable binding orientation, and additionally CB[*n*] is positioned nearer to one Pt center than the other two during the complexation. Thus, all such encapsulation of Pt-based anticancer drugs by CB[*n*] is supported by its (i) hydrophobic cavity and (ii) carbonyl portals which sterically protect them from unnecessary deactivations by biological nucleophiles in our body. Molecular modeling of the complexation of CB[7] with di-Pt (Figure 17) and tri-Pt revealed that they are deeply seated

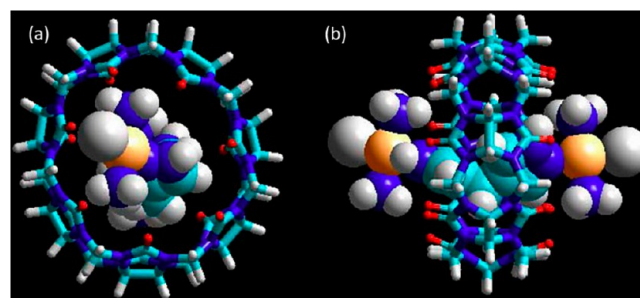


Figure 17. Molecular model illustrating the perfect host-guest encapsulation between di-Pt and CB[7]: (a) top view and (b) side view.¹⁰¹ Reprinted with permission from ref 101. Copyright 2006. The Royal Society of Chemistry.

inside the hydrophobic cavity instead of attaching with the portal.¹⁰¹ Moreover, a slight distortion in CB[*n*] was also observed during the complexation with Pt-based drugs, but the optimal geometry was symmetrical with the methylene protons of dpzm located at the core of CB[*n*]. The center of the cavity of CB[*n*] was concluded to be the zone of maximum shielding, but as soon as the protons are placed near the walls or the portals a slight upfield shift is observed.

2.6. Host-Guest Encapsulation of Histamine Type 2-Receptor Antagonist Ranitidine (11) and CB[7]. Improvement of a smart drug delivery system using CB[7] for the delivery of several drug moieties has truly become the thrust field of research in the pharmaceutical chemistry owing to its excellent host-guest encapsulation capability. Ranitidine hydrochloride (*N,N*-dimethyl-5-[2-(1-methylamino-2-nitrovinylamino) ethylthiomethyl] furfuryl-amine hydrochloride (RH⁺) (Figure 18a) is one such molecule which acts as a histamine H₂ receptor antagonist to inhibit the excess production of stomach acid which can inevitably cause peptic ulcers and other diseases as well.^{102,103} Using UV-visible spectroscopy, it is observed that incorporation of CB[7] into the ranitidine solution at pH 2.5 has led to a decrease in the peaks at 228 and 313 nm (for furanyl protons

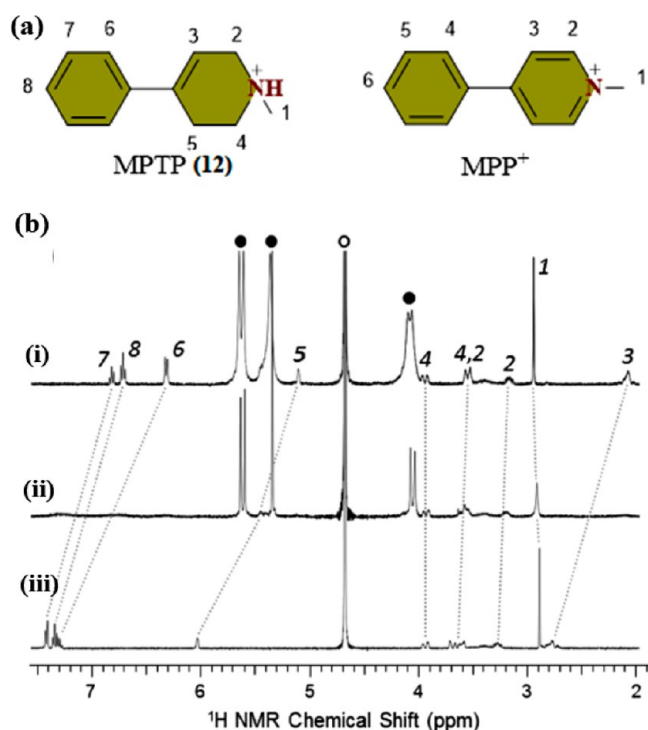


Figure 19. (a) Molecular diagram of MPTP (12) and MPP⁺; (b) ¹H NMR spectral graph showing the resonances of MPTP when encapsulated by (i) 1.2 equiv of CB[7], (ii) 0.5 equiv of CB[7], and (iii) free MPTP. The CB[7] and D₂O protons are indicated by (●) and (○), respectively, in D₂O.¹¹⁶ Reprinted with permission from ref 116. Copyright 2015. The American Chemical Society.

dopamine neurons, thus increasing the production of ROS.¹¹⁷ As a result, there is an immediate need in the development of neuroprotective agents which can restrict the negative impact of neurotoxins in our CNS. ¹H NMR spectral studies have proven perfect host–guest encapsulation of MPTP by CB[7] which is evident from the certain upfield shift (up to ~1.0 ppm, Figure 19b-i) compared to that of the spectrum of uncomplexed MPTP (Figure 19b-ii).¹¹⁶ On incorporating only 0.5 equiv of CB[7], the peaks appeared to be broader along with some disappearance of resonances, which indicates the rate of exchange between the uncomplexed and CB[7]-complexed MPTP.¹¹⁶ Addition of 1.2 equiv of CB[7] ensures perfect host–guest encapsulation inside the CB[7] cavity inferred from the distinct upfield shift of aromatic protons, the ethylene proton in the tetrahydropyridine ring, and the methylene protons.¹¹⁶ The protons adjoining to the nitrogen atom experience only minimal upfield shifts, because they were located close to the carbonyl portal within the cavity.¹¹⁶ One of the methyl protons (H1) experiences downfield shift which was due to its position outside of the cavity nearer to the electron-dense carbonyl-laced portal.¹¹⁶ In fact, one of the methylene protons (H4) did not experience any significant shift upon adding CB[7], which signifies that it is located in such a position that the shielding and the deshielding effect counterbalance each other.¹¹⁶ On increasing the concentration of CB[7], the absorbance peak at 242 nm got attenuated accompanied by a bathochromic shift.¹¹⁶ The DFT study of MPTP-H⁺·CB[7] (Figure 20a) has also proven the same as that of the ¹H NMR study with the two six-membered rings of MPTP well encapsulated inside CB[7] placing the methyl groups outside the cavity near its

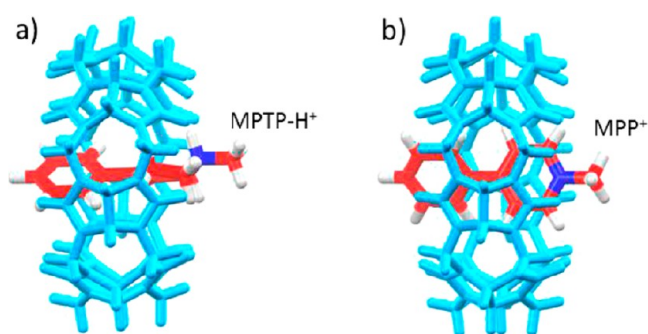


Figure 20. Lateral view of supramolecular encapsulated (a) MPTP-H⁺·CB[7] and (b) MPP⁺·CB[7] based on DFT calculation.¹¹⁶ Reprinted with permission from ref 116. Copyright 2015. The American Chemical Society.

mouth.¹¹⁶ For the MPP⁺·CB[7] complex (Figure 20b), the DFT study is coherent with ¹H NMR study for one of the lowest energies calculated aromatic ring encapsulated within the CB[7] cavity ($\Delta E = 1.6 \text{ kcal}\cdot\text{mol}^{-1}$).¹¹⁶ Mainly, three mechanisms come into the picture while talking about inhibition of neurotoxins by CB[7]. They are the following: (i) CB[7] complexation may hinder MPTP's ability to penetrate the blood–brain barrier to show its neurotoxicity;¹¹⁸ (ii) even if the complex gets through the blood–brain barrier, CB[7] protects the MPTP from oxidation by MAO-B to form active MPP⁺ which mainly inhibits mitochondrial complex I of the electron transport chain and generates ROS;¹¹⁶ (iii) lastly, even if MPP⁺ is still formed, CB[7] restricts the transfer of MPP⁺ to mitochondrial complex I via DAT by mimicking a synthetic receptor.¹¹⁶ Thus, once again the domination of the binding constant between the guest molecule and CB[7] over their biological receptors acts a promising approach toward medicinal chemistry.

2.8. Relocation of Drug by Carrier Protein from the Hydrophobic Nanocavity to Its Binding Pouch—A Host Induced Guest Protonation Approach. To get an insight into the molecular interaction between the supramolecular macrocycles and the drug molecule of interest, basically, two fluorescence-based approaches are present. One is using the inherent optical properties of the drug,³⁶ and another is the use of selective fluorescent dye and studying the tuning of its photophysical properties upon interaction with a water-soluble host and the biomolecule. The second method calls for the dye to be an environment-responsive one for studying the individual binding interaction¹¹⁹ because they show a different fluorescence behavior in different environments. The structural characteristics of these dyes are their intramolecular charge transfer (ICT) properties, and they are composed of two basic components—an electron-rich part (donor) and an electron-deficient part (acceptor) joined by a π -conjugated spacer. They are highly polarity-dependent molecules due to extensive charge transfer.

PRODAN (commonly dubbed as PRO, 13) is a small naphthalene-based ICT fluorescent dye in which 2-*N,N*-dimethyl amino acts as a donor and the 6-propanoyl group acts as an acceptor part (Figure 21). In pH-dependent binding studies of PRO, at basic pH (ca. 9.0), an intense fluorescence enhancement is observed along with a ~35 nm hypsochromic effect, whereas at lower pH (<7.5), fluorescence quenching is observed. In the presence of CB[7], a

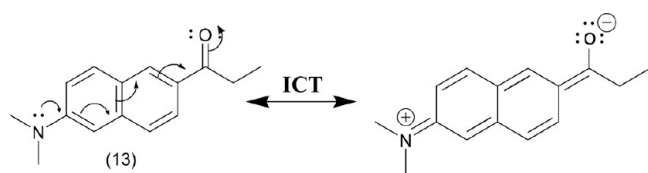


Figure 21. Structure of PRO.

significant pK_a shift was observed (approximately 3.2 units) for both ground and excited states. The fluorescence-based relocation of PRO by 1,6-diamino hexane, a strong competitor of CB[7], confirms perfect encapsulation of PRO in the CB[7] cavity. UV-vis spectroscopy-based binding titration of 10 μM PRO (as above 20 μM self-aggregation occurs) with CB[7] at pH 9.0 reveals the severe diminishing effect on absorption maxima at longer wavelengths around 370 nm and a slight elevation at smaller wavelengths. The isosbestic point at around 290 nm indicates a 1:1 complex formation consistent with the cavity dimension. This fact is strongly supported by the Benesi-Hildebrand plot.¹²⁰ A strong fluorescence quenching is exhibited by adding only 2.5 μM of CB[7] at pH 3.0 (Figure 22a) at 290 nm excitation, which suggests a firm binding conjoined with protonation of the PRO because of the host-induced guest protonation. The binding strength was estimated to be $(2.3 \pm 0.5) \times 10^6 \text{ M}^{-1}$. This fluorescence intensity can again be regenerated by displacing PRO with 1,6-diamino hexane at pH 3.0 (Figure 22b), which further supports the stronger binding of PROH⁺ in CB[7] than PRO. A marked increase in the fluorescence lifetime of PRO was detected in addition to the enhancement of fluorescence intensity from steady-state measurement upon encapsulation with CB[7] which experienced an alleviation of both radiative and nonradiative phenomena. The displacement of PRO in various microenvironments of host macrocycles not only shield PRO from quenching by solvent molecules but also provide a low polarizable inner cavity to PRO giving rise to both longer fluorescence lifetime and reduction of the radiative process (about 1.6 times). The anisotropy decay of the PRO-CB[7] complex is much smaller than the free PRO giving a τ_r value of 0.78 ns, which is shown in Figure

23a (absence of CB[7]) and Figure 23b (presence of CB[7]), which signifies a firm inclusion complex between CB[7] and PRO.

To study the displacement of PRO from the CB[7] nanocavity to the macrocyclic guest binding pouch, competitive biosupramolecular assay was executed where HSA (human serum albumin) and BSA (bovine serum albumin), a highly abundant blood protein, play the role of a stronger competitor which can knock out PRO from the CB[7] cavity very easily and bind it in its hydrophobic pocket (Figure 24a). Upon CB[7] binding, a strong attenuation of fluorescence intensity was observed when excited at 340 nm (Figure 24b) but on gradual addition of a stock solution of HSA shows an appreciable increment of fluorescence intensity (Figure 24c) followed by a 60 nm hypsochromic effect. Thus, this fluorescence activity gives an idea of a relocation phenomenon of PRO from the cavity of a drug delivery vehicle to the blood protein cavity opening a new dimension of research interest in the domain of drug carriers using CB[7] macrocycles.

2.9. In Vivo and In Vitro Study of Cytotoxicity of CB[7] in the Pharmaceutical Field. CB[7] is increasingly in demand for several potential medicinal applications as it imparts several beneficial properties in the wide category of drug molecules, which is much needed in smart drug delivery applications. Its low cytotoxicity acts as an attribute which is motivating chemists to explore its wide variety of applications by mimicking it as a smart nanodrug carrier inside the human body. The CB[7]-induced cytotoxicity was studied by MTT (3-(4,5-dimethylthiazol-2-yl)-2,5-diphenyltetrazolium bromide) assay by incorporating it in Chinese hamster ovary (CHO-K1) cells.¹²¹ To find out the subtoxic dosage of CB[7], a wide range of concentration of CB[7] (0.1–4.5 mM) is dissolved in the cell culture incubated with CHO-K1 cells for about 48 h.¹²¹ If the concentration is above 2 mM, cell growth is found to be inhibited, whereas concentrations up to 1 mM are found to be suitable for the biological cells.¹²¹ To report the exact concentration of CB[7] that will show cytotoxic effects, a broad subtoxic range of up to 1 mM was incubated for the same period of 2 days (Figure 25a), against a control sample without CB[7], which gave an input of an IC_{50} value of $0.53 \pm 0.02 \text{ mM}$.¹²¹ At concentration of

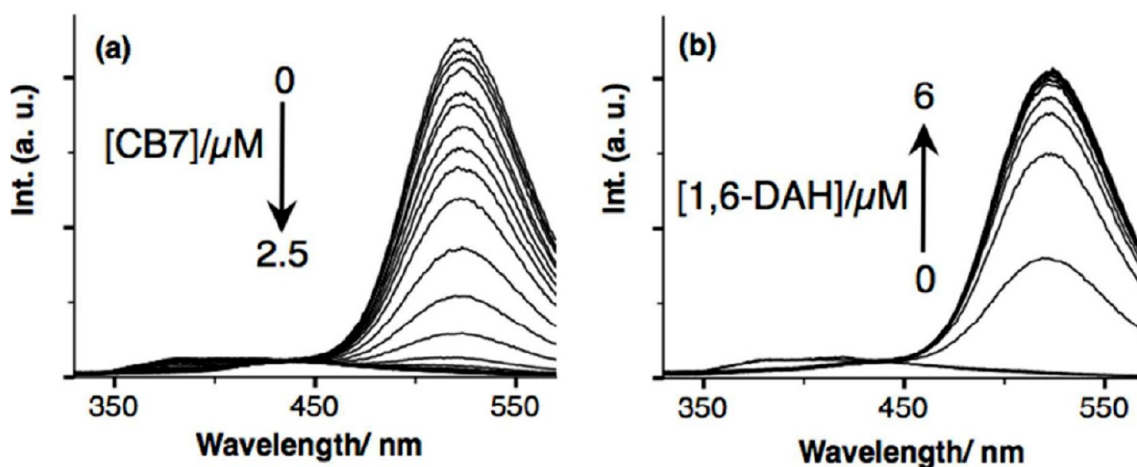


Figure 22. (a) Fluorescence titration plot of 10 mM PRO with increasing CB[7] concentration up to 2.5 μM ; (b) guest relocation assay based on fluorescence titration upon addition of 1,6-diaminohexane in the predeveloped PRO-CB[7] complex.¹²⁰ Reprinted with permission from ref 120. Copyright 2016. The Royal Society of Chemistry.

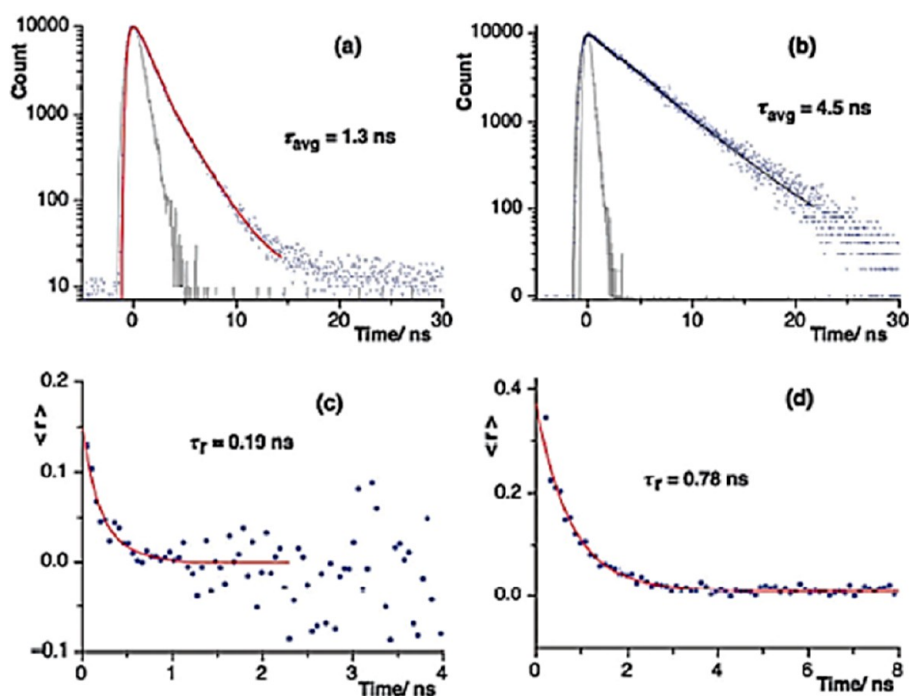


Figure 23. Fluorescence lifetime decay for (a) free and (b) PRO encapsulated CB[7]; bold lines represent the curves of best fitting. Time-resolved anisotropy decay measurement of (c) free PRO molecule and (d) CB[7]·PRO complex.¹²⁰ Reprinted with permission from ref 120. Copyright 2016. The Royal Society of Chemistry.

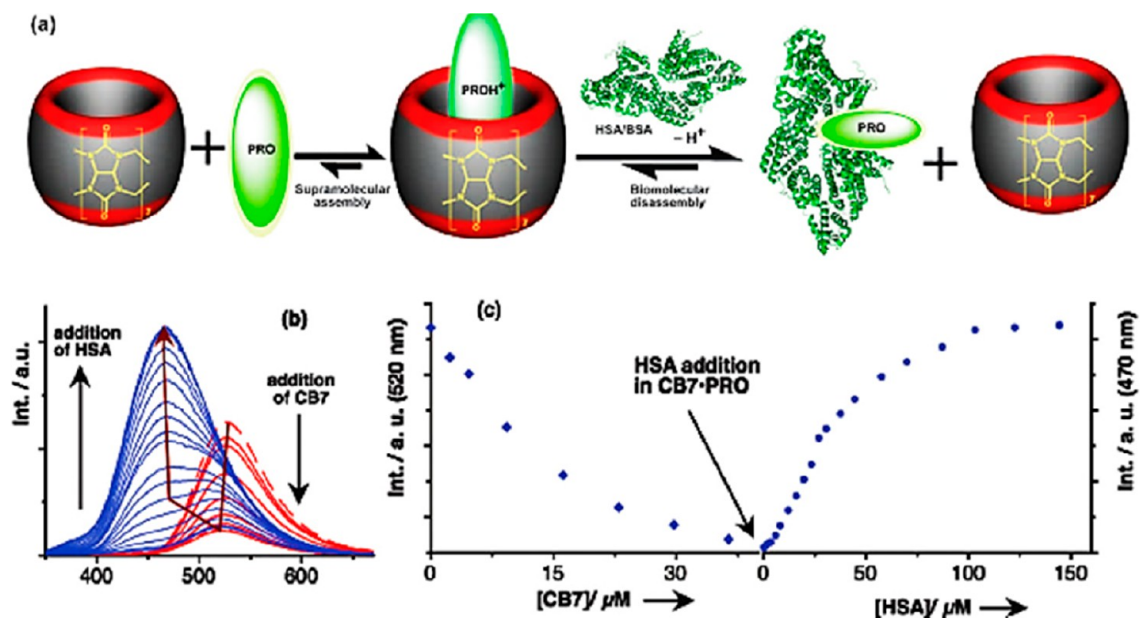


Figure 24. (a) Relocation mechanism of guest molecule PRO by competitor HSA/BSA from the CB[7] cavity; (b) fluorescence-based titration of PRO with increasing concentration of CB[7] up to 36 μM followed by subsequent incorporation of HSA in the predeveloped PRO-CB[7] complex showing a gradual increase in fluorescence intensity reaching a plateau at $\lambda_{\text{ex}} = 340 \text{ nm}$; (c) plot representing the fluorescence intensity against the increasing concentration of CB[7] or HSA at 520 nm for CB[7] and 470 nm for HSA, respectively.¹²⁰ Reprinted with permission from ref 120. Copyright 2016. The Royal Society of Chemistry.

20 μM when incubated in cell culture for 48 h, the cell activity is reduced to $86 \pm 7\%$.¹²¹ The cytotoxic effect of CB[7] was also determined within 3 h of incorporation (Figure 25b), which has assured the absence of any cytotoxicity.¹²¹ In fact, a high concentration of 1 mM of CB[7] has exhibited a tolerance level for the cells at shorter incubation periods. No detrimental effects were seen in mitochondrial activity of CHO-K1 cells stained with

MitoTracker Red CMXRos when incubated with 0.5 mM of CB[7].¹²¹ Moreover, the mitochondria showed intact structure and intact membrane potential when treated with various subtoxic CB[7] concentrations. For in vivo toxicity study, the impact of a single intravenous dose of CB[7] on mice was explored at dose levels up to 300 mg kg^{-1} .¹²¹ No cytotoxicity was observed below a 200 mg kg^{-1} level of dose.¹²¹ However, at elevated dose level and swift injection,

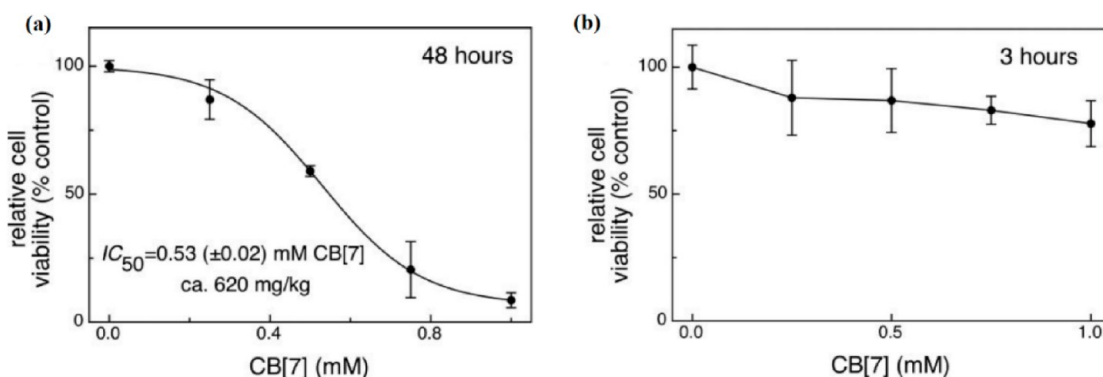


Figure 25. Relative cell viability of CHO-K1 cells in the presence of CB[7] of concentration (0–1 mM) at different incubation times, (a) 48 h and (b) 3 h, measured using the MTT assay by examining formazan absorbance at 570 nm.¹²¹ Reprinted with permission from ref 121. Copyright 2010. The Royal Society of Chemistry.

the mice suffered from a shocklike state just after its administration. The highest tolerated dosage level of CB[7] was reported to be 250 mg kg^{-1} when the injection was pushed at a slow intravenous rate.¹²¹ All the mice injected slowly with the CB[7] began to recover after 5–8 days which signifies the removal of CB[7] from the mice bodies through either excretion or any other means. However, for oral intake the toxicity seems to be negligible in comparison with the intravenous push. Perhaps this is due to the decrease in absorption of CB[7] in the gastrointestinal tract or the lesser tendency to degrade in the oral route.

3. PILLARARENES

3.1. SDDS Based on Pillararenes: Architecture and Its Applications. SDDS using pillararenes is currently a novel rapid developing arena of research due to certain interesting intrinsic features of pillararenes as a drug delivery vehicle. Pillararenes can be fabricated and functionalized very easily, and their certain attributes like immense electron richness, size adjustment, hydrophobic cavity, and single to multistimuli responsiveness can aid to develop suitable host–guest complexes, supramolecular amphiphiles with or without polymer conjugates, supramolecular vesicles, and pillararene-based polymersomes. Functionalization of pillararenes with polymeric conjugates like poly(ethylene glycol) (PEG), poly(*N*-isopropylacrylamide) (PNIPAM), poly(glutamamide) (PGA), and poly(caprolactone) (PCL) enhance the ability to assemble into better nanoaggregates which exhibit excellent host–guest complexation. The most fundamental SDD vehicle based on pillararenes is using it as a nanocontainer with its rim either anionically (carboxylate or phosphate) or cationically (ammonium) ionized encapsulating several oppositely charged guest molecules through electrostatic interaction.^{122–125} The hydrophobic inner cavity of pillararenes potentially increases water solubility and the therapeutic activity inside our biological system. The most commonly known water-soluble pillararenes are carboxylated pillar[5]-arene (CP[5]) and carboxylated pillar[6]arene (CP[6]), which can easily encapsulate NHM (Figure 26) by increasing the solubility factor of NHM by 100 and reducing its cell toxicity significantly.

Yu, and co-workers found out that CP[6] can enhance the solubility of camptothecin (CPT) and hydroxycamptothecin (HCPT) by 380 and 40 times respectively, and their bioactivities of CPT and HCPT substantially became better

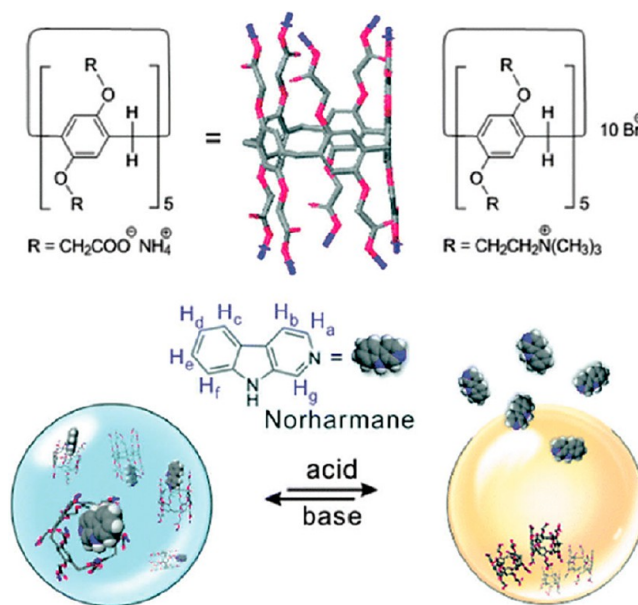


Figure 26. Schematic pictogram of the chemical structure and host–guest complexation between CP[5] and NHM.¹²⁶ Reprinted with permission from ref 126. Copyright 2018. The Royal Society of Chemistry.

as a result of the solubility enhancement.¹²⁸ Tamoxifen (T), a sparingly water-soluble estrogen agonist for breast cancer treatment, also experienced the same advantage. Among the cationic charged cargoes, oxaliplatin (OxPt, 14), an anticancer drug approved by the FDA, has some limitations like low bioavailability, easy degradation before reaching the target, and lack of selectivity of tumor cells which can be easily overcome by host–guest complexation by CP[6] with high binding affinity at pH 7.4 rather than pH 5.4 (ca. 24 times higher). Thus, it can induce the sustained release of the drug in the acidic environment of the tumor (enriched with lactic acid and CO_2) without any toxicity. This type of anticancer drug can be easily released (Figure 27) by a competitor guest which can knock out the desired drug from the cavity at the site of an overexpressed competitor, for example, spermine (SPM), which is a biomarker overexpressed in lungs and colorectal cancer.

PDT, a noninvasive and promising therapeutic approach toward cancer treatment, is often limited by severe drawbacks like dark toxicity, photobleaching effect, and hydrophobicity

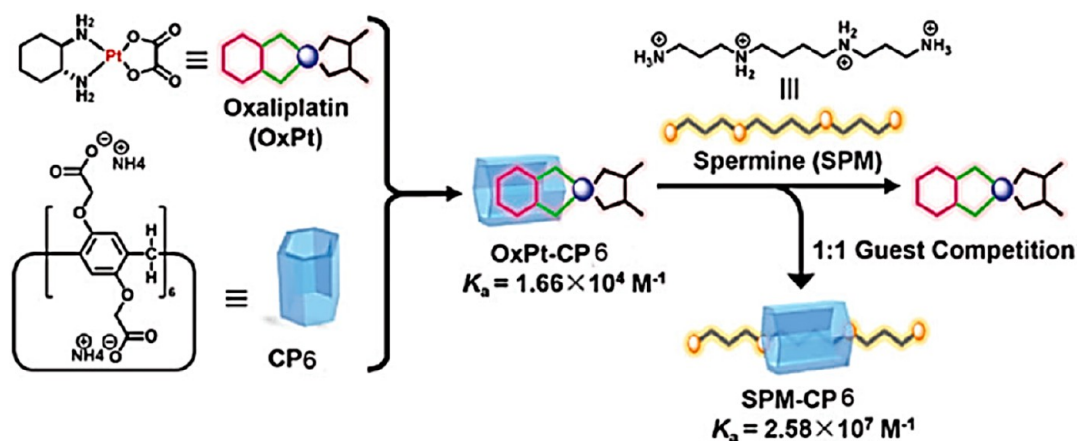


Figure 27. Schematic representation of chemotherapy based on supramolecular host–guest encapsulation between OxPt (14) and CP6.¹²³ Reprinted with permission from ref 123. Copyright 2018. The American Chemical Society.

which can be overcome by using an amphiphilic cationic phenothiazinium molecule, methylene blue (MB, 15), encapsulated in CP[6] (Figure 28). Such encapsulation can

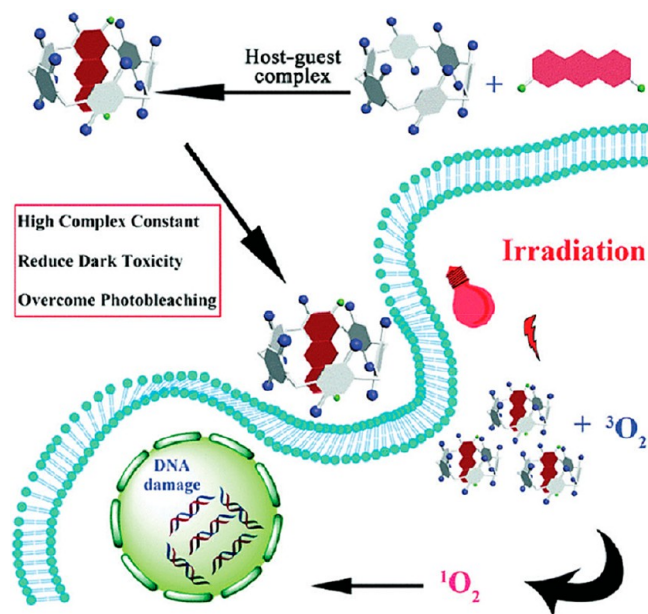


Figure 28. Schematic diagram representing the formation of the supramolecular photosensitizer based on the host–guest complexation between CP[6] and methylene blue (15) for PDT.¹²⁵ Reprinted with permission from ref 125. Copyright 2018. The Royal Society of Chemistry.

result in a long-time ROS generation upon light irradiation responsible for killing cancer cells. Amikacin responsible for killing Gram-negative and Gram-positive bacteria has a higher MIC value which can lead to acute side effects overshadowing its potential therapeutic efficacy. Thus, CP[5] can be a promising drug delivery vehicle for tetracationic amikacin disulfate salt because of noncovalent interactions synergistically contributing toward the pillararene–amikacin complexation process. As a result, the transportation of the drug becomes smarter and more effective.

3.2. Self-Assembly of Amphiphilic Pillararene.

Amphiphilic pillararenes are formed by changing the two mouths of each fag end of hydrophobic cores of pillararene.

Ferrocenium-capped amphiphilic PA[5] can self-aggregate into cationic vesicles responsible for delivery of glutathione (GSH)-responsive drug and siRNA codelivery due to the redox-responsive cationic ferrocenium group.¹²⁶ It is the first self-assembly-based SDDS (Figure 29)

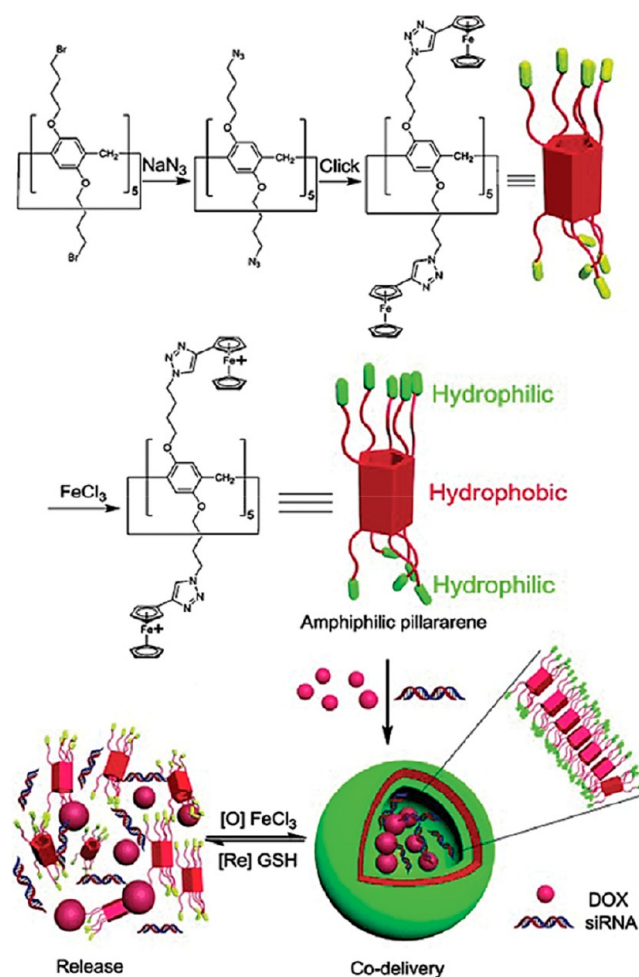


Figure 29. Representation of the fabrication of an amphiphilic PA[5] capped by ferrocene, formation of cationic vesicles, and their redox-responsive drug/siRNA release.¹²⁷ Reprinted with permission from ref 127. Copyright 2014. Wiley-VCH.

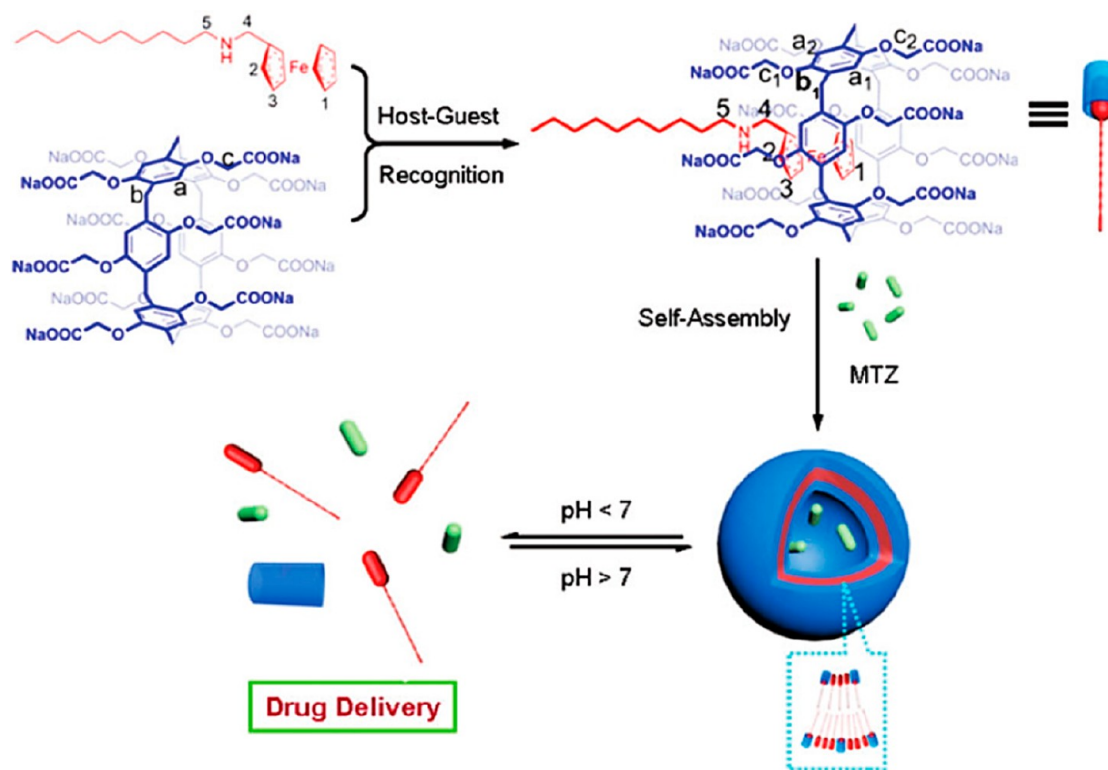


Figure 30. Schematic illustration of pH-sensitive SDDS constructed by complexing CP[6] and FcA (16) to form MTZ (17)-loaded supra-amphiphilic CP[6]-FcA.¹²⁹ Reprinted with permission from ref 129. Copyright 2013. The American Chemical Society.

3.3. Single Stimuli-Responsive SDDS Based on Pillararene. The different pH values of organs, tissues, inflammatory cells, and tumors provide a suitable bait for the pillararene-loaded drugs to be triggered to release at the proper site of action. Thus, this phenomenon provides an incentive to develop intrinsic pH-sensitive SDDSs featuring CP[6] and CP[5], which can rush to the tumor cells in search of an acidic microenvironment for protonating their carboxylate groups fabricated at the rims. In 2012 Huang and co-workers¹²⁸ developed the first PA-based supramolecular vesicles using water-soluble pillar[6]arene (WP[6]) and a pyridine derivative, which showed a reversible interconversion between vesicles and nanotubes in varying pH environments because of the pH-responsiveness of WP[6]. Another pH-sensitive SDS was fabricated by Wang et al.¹²⁹ with an alkyl chain attached with a ferrocene derivative (FcA, 16), which can efficaciously bind CP[6] in water to achieve a tadpole-like supra-amphiphile (CP[6]-FcA). This inclusion complex can further encapsulate the hydrophilic anticancer drug mitoxantrone (MTZ, 17) by curbing the toxicity that the free MTZ drug exhibits to normal cells. Although the drug-loading efficiency is too low (11.2%), it exhibited timely release at a low pH environment (Figure 30). Such application paves the way toward potential anticancer treatment. In 2017 selenium-containing PA[5] was synthesized.¹³⁰ The selenoxide group adds redox responsiveness to the host-guest complexation and forms water-insoluble P[5]Se. This vesicular structure can undergo reversible disassembly/assembly process and can be used for the sustained release of DOX for anticancer therapy for about 84% in 24 h upon addition of vitamin C reducing hydrophobic selenium to hydrophilic selenide. Thus,

morphological tuning is used for triggering sustained anticancer drug release.

3.4. Multiple Stimuli-Responsive SDDS Based on Pillararene. Apart from single stimuli-responsive SDDS, rational designs to develop multistimuli-responsive drugs where response other than the pH is introduced will be a pioneering landmark in the field of drug delivery systems. Apart from pH stimuli, light stimulus is a special stimulus of interest due to its noninvasive nature, cleanliness, controllability, and rapidness.¹³⁰ Azobenzene, being a famous photoresponsive molecule, finds immense application in several modern host-guest systems. Huang et al. reported supramolecular vesicles (SVs) assembled from water-soluble PA[6] and an azobenzene guest in water¹³¹ in which both UV and visible light irradiation can modulate reversible transformation between SVs and nanoparticles pertaining to the photoresponsive characteristics of the azobenzene molecule. The disulfide bond can also play the role of copartner with pH stimuli because the disulfide bond is a glutathione (GSH)-responsive group where lysine derivative (LysD) acts as a guest and dual GSH- and pH-responsive supramolecular vesicles act as a host which in turn form a strong inclusion complex. This can strongly encapsulate MTZ and exhibit its rapid release at the acidic environment of the tumor with high GSH concentration as GSH cleaves the disulfide bond.¹³² Thus, MTZ-packed vesicles can potentially suppress the proliferation of HepG2 cancer cells. PA[n]s modified with phosphate substituents can further enhance biocompatibility which is used to form amphiphilic host-guest complex using WP[5]P as a host and pyridinium bromide as a guest whereas hollow SVs can be prepared from WP[6]P and pyridinium bromide guest (Figure 31). Both are pH-responsive and Zn²⁺-responsive. The supramolecular

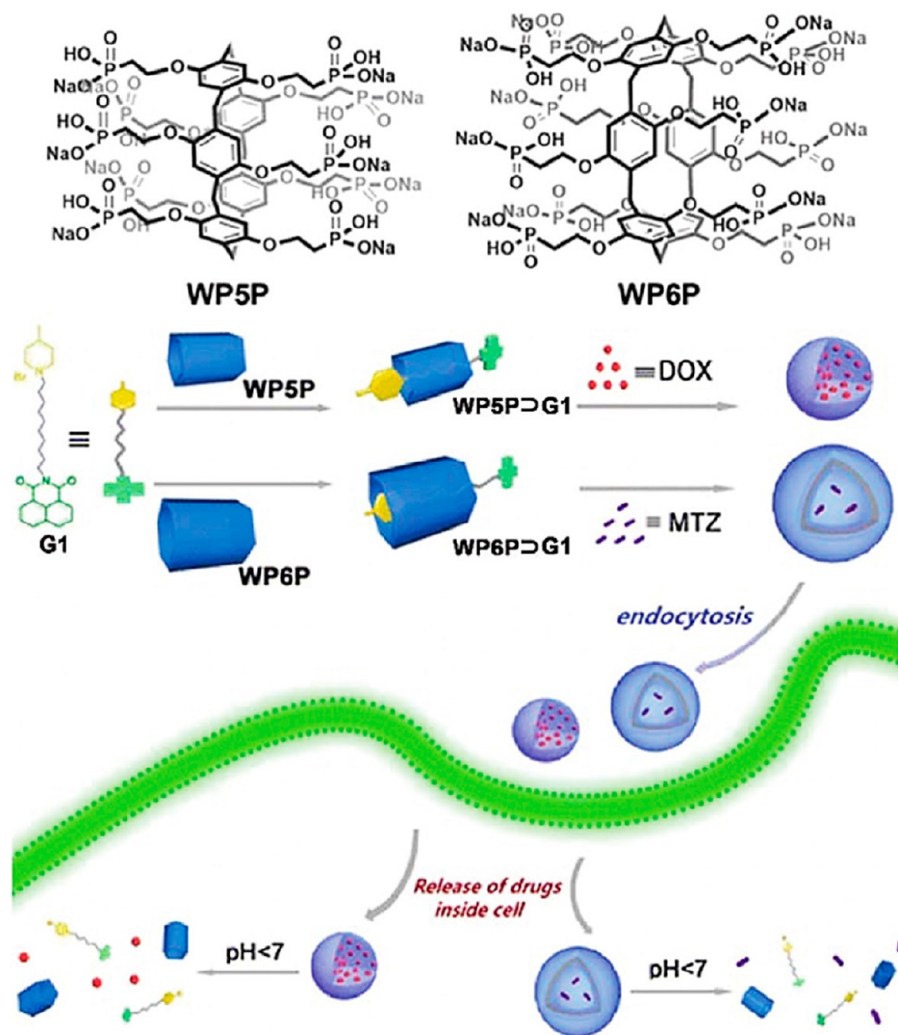


Figure 31. Schematic representation of the construction of the amphiphilic host–guest complex developed from WP[5]P as a host and pyridinium bromide as a guest; hollow SVs can be prepared from WP[6]P and pyridinium bromide guest.¹³³ Reprinted with permission from ref 133. Copyright 2016. The American Chemical Society.

micelle can load the hydrophobic anticancer drug doxorubicin (DOX), but the latter one can encapsulate MTZ. Saint molecules (pyridinium amphiphiles composed of one pyridinium moiety and two alkyl chains), potential vectors for intracellular delivery of DNA, and WP[6] can together form multifunctional supramolecular vesicles which are pH, Ca^{2+} , and thermal responsive (Figure 32).¹³⁵ Cationic Saint complex can cause blood clots during drug delivery, so that is why by encapsulating the Saint molecule, the pyridinium moiety get rooted inside the cavity of WP[6] that can be remodelled into anionic self-assembled vesicles by the 12-carboxylate group of WP[6]. Upon introducing Ca^{2+} , the vesicle can undergo disruption and by increasing the temperature around 36 °C led to the generation of a large-sized vesicle which will be useful for biomimetic and bioimaging application. Thus, this host–guest complexation can easily remove all the backlogs of the Saint molecule. Novel CO_2 -responsive SVs can be developed from a PA[5] and an anionic surfactant, sodium dodecyl sulfonate (SDS).¹³⁵ The SVs can be reversibly destroyed just by temperature treatment or by bubbling N_2 to remove CO_2 and again restoring upon bubbling with CO_2 . This is also a dual

stimulus-responsive SV capable of loading the water-soluble dye Calcein.

3.5. Stimuli-Responsive SDDS Based on Pillararene for Dual Therapy. Besides surgery, chemotherapy is also a main strategy for treating cancer, but its several side effects and drug resistance overshadow its anticancer efficacy. So, to get over these shortcomings, the so-called “combined therapy” is introduced, which includes numerous therapies like combination of chemotherapy (CT) and photodynamic therapy (PDT), photothermal therapy (PTT), or both. To investigate the benefits of combined therapy, a light-harvesting system designed with boron-dipyrromethene (BODIPY, a widely used ideal photosensitizer) modified with a quaternary ammonium derivative dye was employed as a guest to complex with CP[5].¹³⁶ BODIPY has a high absorption coefficient and high ROS yield suitable for PDT.¹³⁷ The complex further self-assembles into supramolecular vesicles, which firmly encapsulate the anticancer drug DOX with high loading efficiency and sustain release in acidic pH leading to the pioneering epitome of a pillararene-based supramolecular nanocarrier for effective chemo-photodynamic dual therapy. Moreover, the DOX-loaded vesicles can well localize in lysosomes and exhibit an incredible fusion

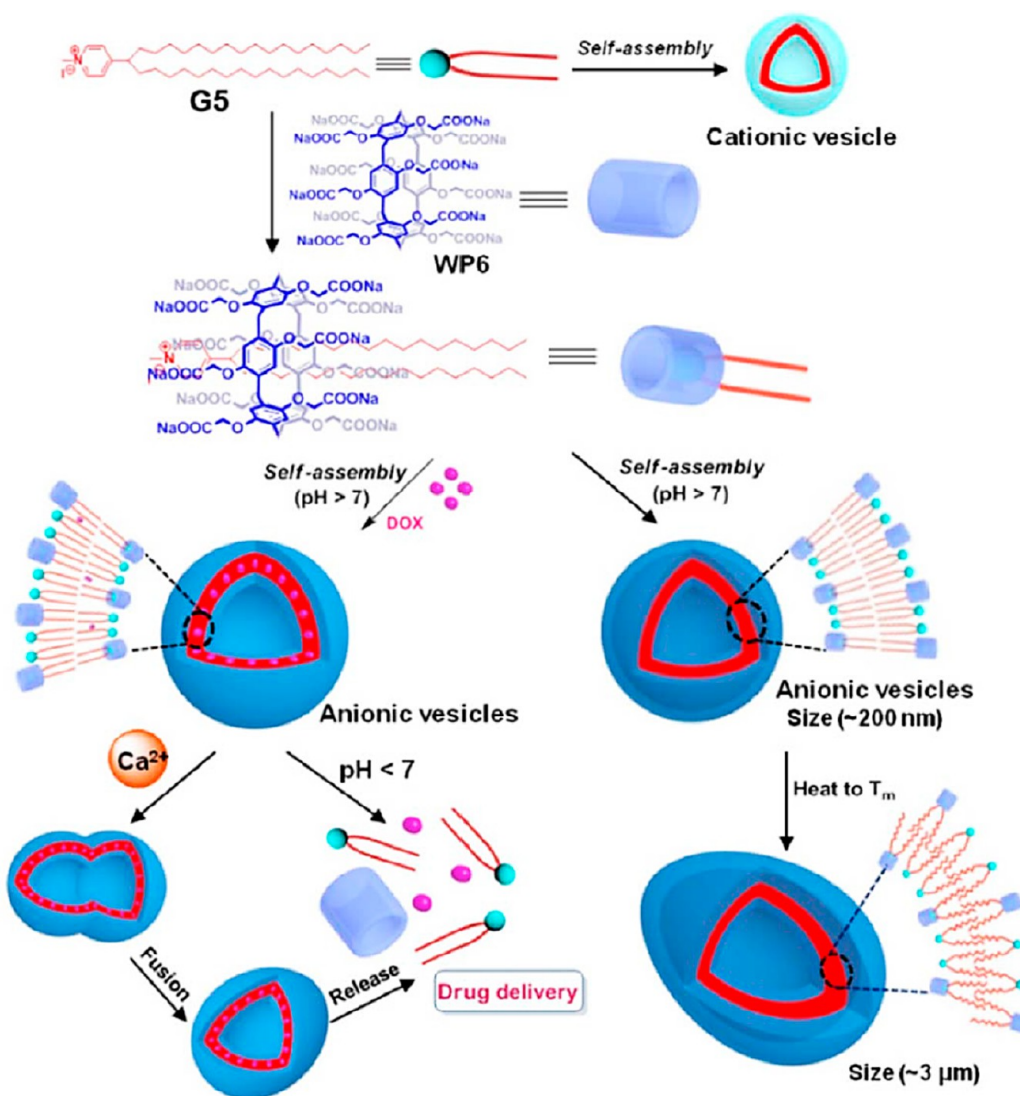


Figure 32. Schematic representation of the formation of multistimuli-responsive SVs fabricated from WP[6] and Saint molecule.¹³⁴ Reprinted with permission from ref 134. Copyright 2014. The American Chemical Society.

of chemo- and photodynamic activities against A549 cancer cells upon irradiating with red light, highlighting the potentiality of DDS for chemo-photodynamic dual therapy.

3.6. Fabrication of Stimuli-Responsive SDDS from Pillararene Based on Pro-drug Strategy. In the journey of developing smart nanocarriers for drug delivery, these smart drug vehicles experienced several intrinsic drawbacks like low drug-loading capacity and premature burst release which restrict their usages. So, a pro-drug approach is used where a parent drug is connected to a macromolecule. It is pharmacologically inactive and requires enzymatic or stimuli-responsive transformation when it arrives at its target site. DOX-based pro-drugs were designed directly connecting hydrophobic DOX with a pyridinium-functionalized flexible alkyl chain or a short EGN (ethylene glycol) chain via a hydrazone bond which can easily be cleavable by acid within 30 min (Figure 33). CP[6] also catalyzes the cleaving of the hydrazone bond, thus resulting in rapid release of drug molecules under acidic conditions. This type of DOX-based supramolecular pro-drug can enter SKOV3 cancer cells by endocytosis and can lead to its inhibition verified by MTT assay.

Multidrug resistance (MDR) is a major hurdle in the path of successful targeted drug or combination chemotherapy, so to overcome this problem, a new approach is developed toward the construction of a synergistic supramolecular drug carrier via drug–drug conjugate. This drug–drug conjugate is synthesized by taking CP[6] as a host and DOX linked with another pyridine derivative drug, isoniazide, by acid-cleavable bonds like disulfide bonds or hydrazone bonds. This obtained system shows higher drug-loading capacity and accelerated drug release along with immense stability.

3.7. Construction of Pillararene-Based SDDS Using Biomolecules. Tryptophan (Trp), an essential amino acid, is known to interact with DNA through the indole ring. Multiple indole rings of tryptophan can add strength to supramolecular interaction with DNA. After realizing it, Trp-modified PA[5] is synthesized.¹³⁹ The supramolecular vesicle assembled by TP[5] and galactose derivative can encapsulate and carry DOX·HCl (Figure 34), which not only showed hepatoma-targeting capability to asialoglycoprotein receptor (ASGP-R) overexpressed HepG2 cells but also can overcome DOX-resistant hepatoma cells due to significant interaction between TP[5] and DOX·HCL. This is the first synergistic

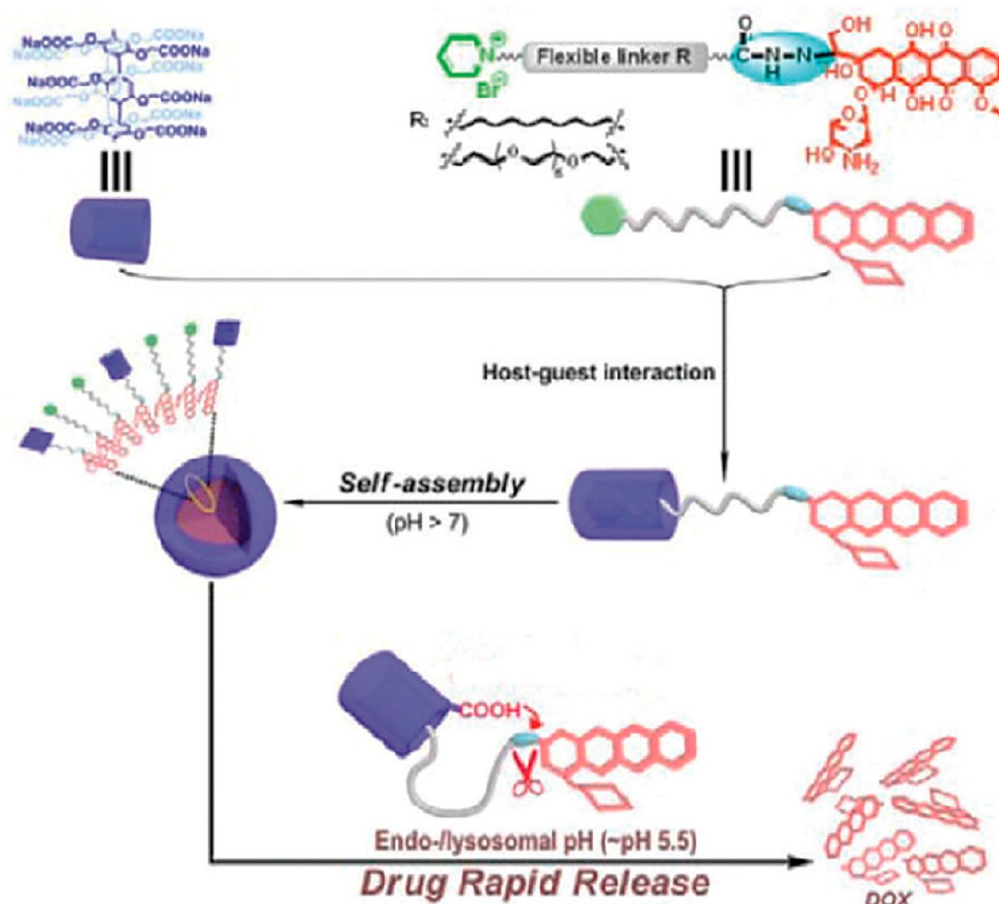


Figure 33. Schematic diagram of the assembly of supramolecular pro-drug nanoparticles based on CP[6] and DOX-based pro-drugs.¹³⁸ Reprinted with permission from ref 139. Copyright 2015. The American Chemical Society.

DNA-interacting drug nanocarrier reported to date. There are many biomolecule-based biocompatible PA[*n*]s like glycopillararene, mannosylated PA[5],¹⁴⁰ and galactosylated PA[5]¹⁴¹ in which the latter finds its application as a host for encapsulating CPT-based pro-drug for cancer treatment.

3.8. Pillararenes-Based SDDS for Treatment of Juvenile Diabetes. Incorporation and delivery of biomacromolecules (enzymes and hormones) via PA[*n*]s SDDS is slightly problematic due to their large size, easy biodegradation, and fragility. For treatment of diabetes mellitus, smart and intelligent SDS loaded with insulin was synthesized through self-assembly of the complex between guest-modified pyridylboronic acid and WP[5] host.¹⁴³ A sudden increase in glucose triggers the release of insulin due to a stronger binding reaction between *cis*-diol and boric acid. Later, to enhance the selectivity and sensitivity of this complex toward glucose, monoboric acid is replaced with diphenylboronic acid bearing a long alkyl chain during guest synthesis. This supra-amphiphile can further undergo self-assembly to form vesicles which are glucose specific and can encapsulate insulin with high efficiency. These novel supramolecular vesicles showed the researchers a bright future for a potential diabetic therapy during hyperglycaemic conditions. Another type of novel insulin-loaded SV was synthesized in which a ditopic phenylboronic acid derivative containing pyrene fluorophore as a biosensor and a trimethylammonium group as a binding site with water-soluble PA[5] which can even self-assemble into vesicles was present.¹⁴⁴ These SVs can encapsulate

insulin and glucose oxidase (GOx) (Figure 35). The pyrene fluorophore stacked in a π - π fashion in the aggregated state yields excimer emission around 470 nm, allowing us to recognize it by the naked eye. When there is an increment in glucose concentration in our body, the ditopic phenylboronic acid will identify and bind glucose, resulting in the oxidation of glucose by GOx to form gluconic acid leading to a decrease in pH and evolution of H₂O₂. This decrease of pH stimulates the protonation of WP[5] and the rupturing of the host-guest interaction, which further collapse the SVs and release insulin. Thus, these SVs mimic a healthy pancreas and deliver insulin during the needs of the body in presence of the excess glucose.

4. CONCLUSION

In conclusion, diverse SDDS based on CB[*n*] and pillararenes are elaborately reviewed in this paper. A variety of strategies are put forward in the field of biomedicine by tuning several hosts or guests which successfully meet different requirements. Nevertheless, the research areas of various CB[*n*] and PA[*n*]-based SDDS are still in infancy, and thus there are extensive scopes of solving existing problems and developing new systems to make the field of drug delivery a truly potential one. Despite many advantages, there are many bottleneck issues faced during the research with these macrocyclic drug delivery systems. Regarding CB[*n*]-based compounds and nanomaterials, Kim et al. showed the nontoxicity of CB[*n*] systems with ED₅₀ level of more than

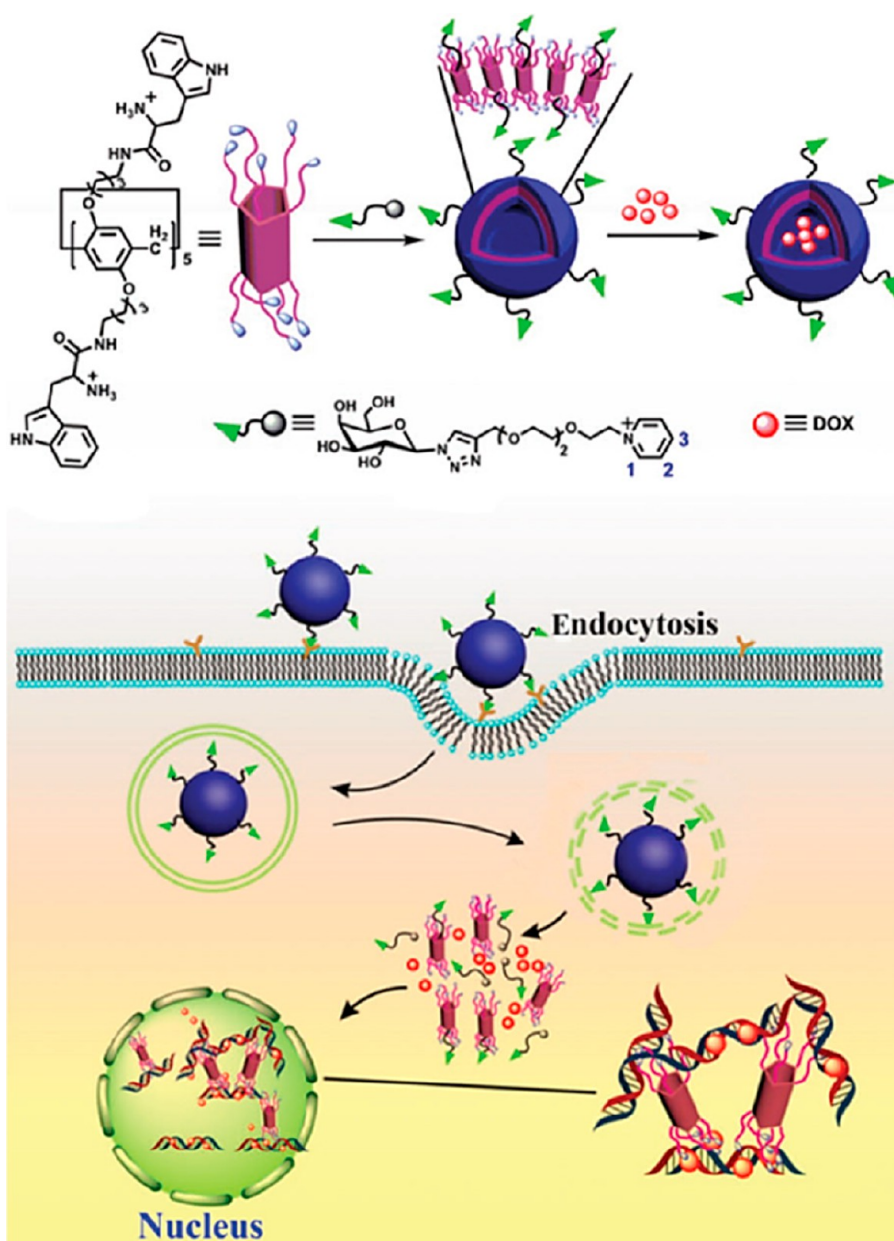


Figure 34. Schematic representation of the formation and drug-loading procedure of a vesicle based on Trp-modified PA[5] and a galactose derivative.¹⁴² Reprinted with permission from ref 143. Copyright 2016. The American Chemical Society.

100 μM against human lung and ovarian cancer cells.¹⁴⁵ Due to low solubility of CB[8], accurate determination of its toxicity level is left undetermined. Another important issue which needs to be considered before using any drug delivery containers is their cell permeability. CB[7] complexes with fluorophores conjoined with spermidine and adamantylamine were demonstrated by Isaacs et al. to be capable of crossing the cell membranes of murine macrophage cells, within 20 min, with 86% of the cells incorporated into the complex.¹⁴⁶ Similarly, many limitations are also faced with pillaranes. High-level pillar[n]arenes ($n > 7$) usually do not have appreciable large-sized cavities because of structural folding and cannot be produced on a massive scale due to the uncompetitive cyclization process.¹⁴⁷ Moreover, two functional groups need to be covalently connected para to each repeating phenylene unit, which immensely hinders their structural diversity and flexibility. In this context, it should be

noted that developing smart nanomaterials for human health is one of the most important aims that chemists have studied. Therefore, implementations of controllable SDDS in practical gene/drug delivery should be a priority forever, and there is no doubt that immense progress will be achieved soon, as much successful research is going on in leaps and bounds much faster than ever predicted, and such smart SDDS will play an immense potential role in the biomedical field.

5. OUTLOOK

Cucurbiturils and pillaranes have unique blends of various supramolecular characteristics which have prepared them to rival other conventional macrocycles in terms of flexible yet targeted drug delivery in human bodies. The arena of this research field has targeted several undiscovered treatments and cures of many deadly diseases like cancer as well as diabetes. Cucurbiturils and pillaranes have acute potential to

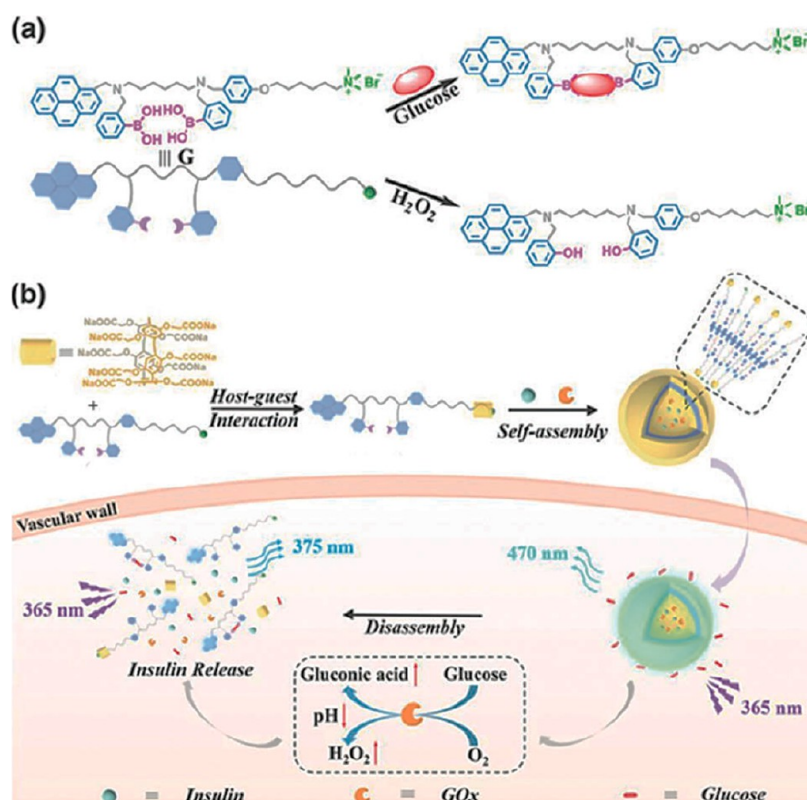


Figure 35. Schematic representation of a glucose-triggered supramolecular insulin transport system. (a) Chemical structure and mechanism of multiresponsiveness of diphenylboronic acid guest molecules. (b) Vesicles formed out of supramolecular self-assembly of the host-guest complex and its efficient insulin release.¹⁴⁴ Reprinted with permission from ref 144. Copyright 2018. Wiley-VCH.

unlock the unknown cures for many ailments due to their drug encapsulation properties. This field has immense areas yet to be cultivated and holds a handful of promises to land a revolution in the field of medicinal chemistry.

AUTHOR INFORMATION

Corresponding Author

Soumyabrata Goswami – Department of Chemistry, Amity University Kolkata, Kolkata, West Bengal 700135, India;
 orcid.org/0000-0002-9646-1439;
 Email: sgoswami423@gmail.com, sgoswamichem@gmail.com

Author

Arnab Roy Chowdhury – Department of Chemistry, Amity University Kolkata, Kolkata, West Bengal 700135, India

Complete contact information is available at:
<https://pubs.acs.org/10.1021/acsomega.3c05465>

Notes

The authors declare no competing financial interest.

ACKNOWLEDGMENTS

S.G and A.R.C thank Amity University Kolkata for infra-structural support. This work did not receive any specific grant from funding agencies in the public, commercial, or not-for-profit sectors.

REFERENCES

- (1) Challa, R.; Ahuja, A.; Ali, J.; Khar, R. Cyclodextrins in drug delivery: An updated review. *Aaps Pharmscitech* **2005**, *6*, E329–E357.
- (2) Da Silva, E.; Lazar, A.; Coleman, A. Biopharmaceutical applications of calixarenes. *J. Drug Deliv Sci. Technol.* **2004**, *14*, 3–20.
- (3) Gillan, R. *Modelling molecules for drug delivery*; Royal Society of Chemistry, Thomas Graham House: Science Park, Milton Road, Cambridge, 2006.
- (4) Hirayama, F.; Uekama, K. Cyclodextrin-based controlled drug release system. *Adv. Drug Delivery Rev.* **1999**, *36*, 125–141.
- (5) Jeon, Y. J.; Kim, S.; Ko, Y. H.; Sakamoto, S.; Yamaguchi, K.; Kim, K. Novel molecular drug carrier: encapsulation of oxaliplatin in cucurbit[7]uril and its effects on stability and reactivity of the drug. *Org. Biomol. Chem.* **2005**, *3*, 2122–2125.
- (6) Montes-Navajas, P.; González-Béjar, M.; Scaiano, J.; García, H. Cucurbituril complexes cross the cell membrane. *Photochem. Photobiol. Sci.* **2009**, *8*, 1743–1747.
- (7) Uekama, K.; Hirayama, F.; Irie, T. Cyclodextrin drug carrier systems. *Chem. Rev.* **1998**, *98*, 2045–2076.
- (8) Wheate, N. J. Improving platinum (II)-based anticancer drug delivery using cucurbit[n]urils. *J. Inorg. Biochem.* **2008**, *102*, 2060–2066.
- (9) Zhao, Y.; Buck, D. P.; Morris, D. L.; Pourgholami, M. H.; Day, A. I.; Collins, J. G. Solubilisation and cytotoxicity of albendazole encapsulated in cucurbit[n]uril. *Org. Biomol. Chem.* **2008**, *6*, 4509–4515.
- (10) Barrow, S. J.; Kasera, S.; Rowland, M. J.; Del Barrio, J.; Scherman, O. A. Cucurbituril-based molecular recognition. *Chem. Rev.* **2015**, *115*, 12320–12406.
- (11) Lagona, J.; Mukhopadhyay, P.; Chakrabarti, S.; Isaacs, L. The cucurbit[n]uril family. *Angew. Chem., Int. Ed.* **2005**, *44*, 4844–4870.

- (12) Masson, E.; Ling, X.; Joseph, R.; Kyeremeh-Mensah, L.; Lu, X. Cucurbituril chemistry: a tale of supramolecular success. *RSC Adv.* **2012**, *2*, 1213–1247.
- (13) Ling, X.; Saretz, S.; Xiao, L.; Francescon, J.; Masson, E. Water vs. cucurbituril rim: a fierce competition for guest solvation. *Chem. Sci.* **2016**, *7*, 3569–3573.
- (14) Nau, W. M.; Florea, M.; Assaf, K. I. Deep inside cucurbiturils: physical properties and volumes of their inner cavity determine the hydrophobic driving force for host-guest complexation. *Isr. J. Chem.* **2011**, *51*, 559–577.
- (15) Gavvala, K.; Sengupta, A.; Hazra, P. Modulation of Photophysics and pKa Shift of the Anti-cancer Drug Camptothecin in the Nanocavities of Supramolecular Hosts. *ChemPhysChem.* **2013**, *14*, 532–542.
- (16) Gavvala, K.; Sengupta, A.; Koninti, R. K.; Hazra, P. Prototypical and photophysical properties of ellipticine inside the nanocavities of molecular containers. *J. Phys. Chem. B* **2013**, *117*, 14099–14107.
- (17) Koninti, R. K.; Sappati, S.; Satpathi, S.; Gavvala, K.; Hazra, P. Spectroscopy and Dynamics of Cryptolepine in the Nanocavity of Cucurbit [7] uril and DNA. *ChemPhysChem.* **2016**, *17*, 506–515.
- (18) Assaf, K. I.; Nau, W. M. Cucurbiturils: from synthesis to high-affinity binding and catalysis. *Chem. Soc. Rev.* **2015**, *44*, 394–418.
- (19) Frischmann, P. D.; Kunz, V.; Würthner, F. Bright Fluorescence and Host-Guest Sensing with a Nanoscale M4L6 Tetrahedron Accessed by Self-Assembly of Zinc-Imine Chelate Vertices and Perylene Bisimide Edges. *Angew. Chem., Int. Ed.* **2015**, *127*, 7393–7397.
- (20) Iqbal, P.; Preece, J. A.; Mendes, P. M. Nanotechnology: The “Top-Down” and “Bottom-Up” Approaches. *Supramolecular chemistry: From molecules to nanomaterials*; Wiley Online Library, John Wiley and Sons: New York, 2012.
- (21) Hu, C.; Lan, Y.; West, K. R.; Scherman, O. A. Cucurbit [8] uril-Regulated Nanopatterning of Binary Polymer Brushes via Colloidal Templating. *Adv. Mater.* **2015**, *27*, 7957–7962.
- (22) Kim, K.; Selvapalam, N.; Ko, Y. H.; Park, K. M.; Kim, D.; Kim, J. Functionalized cucurbiturils and their applications. *Chem. Soc. Rev.* **2007**, *36*, 267–279.
- (23) Xu, X.; Appel, E. A.; Liu, X.; Parker, R. M.; Scherman, O. A.; Abell, C. Formation of cucurbit[8]uril-based supramolecular hydrogel beads using droplet-based microfluidics. *Biomacromolecules.* **2015**, *16*, 2743–2749.
- (24) Chen, G.; Jiang, M. Cyclodextrin-based inclusion complexation bridging supramolecular chemistry and macromolecular self-assembly. *Chem. Soc. Rev.* **2011**, *40*, 2254–2266.
- (25) Hu, Q.-D.; Tang, G.-P.; Chu, P. K. Cyclodextrin-based host-guest supramolecular nanoparticles for delivery: from design to applications. *Acc. Chem. Res.* **2014**, *47*, 2017–2025.
- (26) Li, J.; Loh, X. J. Cyclodextrin-based supramolecular architectures: syntheses, structures, and applications for drug and gene delivery. *Adv. Drug Delivery Rev.* **2008**, *60*, 1000–1017.
- (27) Nangung, R.; Lee, Y. M.; Kim, J.; Jang, Y.; Lee, B.-H.; Kim, I.-S.; Sokkar, P.; Rhee, Y. M.; Hoffman, A. S.; Kim, W. J. Polycyclodextrin and poly-paclitaxel nano-assembly for anticancer therapy. *Nat. Commun.* **2014**, *5*, 1–12.
- (28) Wang, K.; Liu, Y.; Li, C.; Cheng, S.-X.; Zhuo, R.-X.; Zhang, X.-Z. Cyclodextrin-responsive micelles based on poly (ethylene glycol)-polypeptide hybrid copolymers as drug carriers. *ACS Macro Lett.* **2013**, *2*, 201–205.
- (29) Yan, Q.; Yuan, J.; Cai, Z.; Xin, Y.; Kang, Y.; Yin, Y. Voltage-responsive vesicles based on orthogonal assembly of two homopolymers. *J. Am. Chem. Soc.* **2010**, *132*, 9268–9270.
- (30) Guo, D.-S.; Liu, Y. Supramolecular chemistry of p-sulfonatocalix [n] arenes and its biological applications. *Acc. Chem. Res.* **2014**, *47*, 1925–1934.
- (31) Nimse, S. B.; Kim, T. Biological applications of functionalized calixarenes. *Chem. Soc. Rev.* **2013**, *42*, 366–386.
- (32) di Nunzio, M. R.; Agostoni, V.; Cohen, B.; Gref, R.; Douhal, A. A “ship in a bottle” strategy to load a hydrophilic anticancer drug in porous metal organic framework nanoparticles: efficient encapsulation, matrix stabilization, and photodelivery. *J. Med. Chem.* **2014**, *57*, 411–420.
- (33) Horcajada, P.; Gref, R.; Baati, T.; Allan, P. K.; Maurin, G.; Couvreur, P.; Ferey, G.; Morris, R. E.; Serre, C. Metal-organic frameworks in biomedicine. *Chem. Rev.* **2012**, *112*, 1232–1268.
- (34) Meek, S. T.; Greathouse, J. A.; Allendorf, M. D. Metal-organic frameworks: A rapidly growing class of versatile nanoporous materials. *Adv. Mater.* **2011**, *23*, 249–267.
- (35) Kemp, S.; Wheate, N. J.; Stootman, F. H.; Aldrich-Wright, J. R. The host-guest chemistry of Proflavine with cucurbit[6, 7, 8]urils. *Supramol. Chem.* **2007**, *19*, 475–484.
- (36) Mohanty, J.; Bhasikuttan, A.; Nau, W.; Pal, H. Cucurbituril Encapsulation of Fluorescent Dyes. *J. Phys. Chem. B* **2006**, *110*, 5132.
- (37) Moon, K.; Kaifer, A. E. Modes of binding interaction between viologen guests and the cucurbit [7] uril host. *Org. Lett.* **2004**, *6*, 185–188.
- (38) Song, Y.; Huang, X.; Hua, H.; Wang, Q. The synthesis of a rigid conjugated viologen and its cucurbituril pseudorotaxanes. *Dyes Pigm.* **2017**, *137*, 229–235.
- (39) Hennig, A.; Bakirci, H.; Nau, W. M. Label-free continuous enzyme assays with macrocycle-fluorescent dye complexes. *Nat. Methods* **2007**, *4*, 629–632.
- (40) Nau, W. M.; Ghale, G.; Hennig, A.; Bakirci, H. S.; Bailey, D. M. Substrate-selective supramolecular tandem assays: monitoring enzyme inhibition of arginase and diamine oxidase by fluorescent dye displacement from calixarene and cucurbituril macrocycles. *J. Am. Chem. Soc.* **2009**, *131*, 11558–11570.
- (41) Wang, Q.; Barge, L. M.; Steinbock, O. Microfluidic production of pyrophosphate catalyzed by mineral membranes with steep pH gradients. *Eur. J. Chem.* **2019**, *25*, 4732–4739.
- (42) Klöck, C.; Dsouza, R. N.; Nau, W. M. Cucurbituril-mediated supramolecular acid catalysis. *Org. Lett.* **2009**, *11*, 2595–2598.
- (43) Ogoshi, T.; Kanai, S.; Fujinami, S.; Yamagishi, T.-A.; Nakamoto, Y. para-Bridged symmetrical pillar [5] arenes: their Lewis acid catalyzed synthesis and host-guest property. *J. Am. Chem. Soc.* **2008**, *130*, 5022–5023.
- (44) Wang, Y.; Ping, G.; Li, C. Efficient complexation between pillar[5]arenes and neutral guests: from host-guest chemistry to functional materials. *ChemComm.* **2016**, *52*, 9858–9872.
- (45) Sun, Y. L.; Yang, Y. W.; Chen, D. X.; Wang, G.; Zhou, Y.; Wang, C. Y.; Stoddart, J. F. Mechanized silica nanoparticles based on pillar [5] arenes for on-command cargo release. *Small* **2013**, *9*, 3224–3229.
- (46) Yao, Y.; Xue, M.; Chen, J.; Zhang, M.; Huang, F. An amphiphilic pillar [5] arene: synthesis, controllable self-assembly in water, and application in calcein release and TNT adsorption. *J. Am. Chem. Soc.* **2012**, *134*, 15712–15715.
- (47) Zhang, H.; Ma, X.; Nguyen, K. T.; Zhao, Y. Biocompatible pillararene-assembly-based carriers for dual bioimaging. *ACS Nano* **2013**, *7*, 7853–7863.
- (48) Fan, J.; Deng, H.; Li, J.; Jia, X.; Li, C. Charge-transfer inclusion complex formation of tropylium cation with pillar[6]-arenes. *ChemComm.* **2013**, *49*, 6343–6345.
- (49) Han, C.; Xia, B.; Chen, J.; Yu, G.; Zhang, Z.; Dong, S.; Hu, B.; Yu, Y.; Xue, M. A pillar [5] arene-based anion responsive supramolecular polymer. *RSC Adv.* **2013**, *3*, 16089–16094.
- (50) Li, C.; Ma, J.; Zhao, L.; Zhang, Y.; Yu, Y.; Shu, X.; Li, J.; Jia, X. Molecular selective binding of basic amino acids by a water-soluble pillar[5]arene. *ChemComm.* **2013**, *49*, 1924–1926.
- (51) Yao, H.; Wang, Y. M.; Quan, M.; Farooq, M. U.; Yang, L. P.; Jiang, W. Adsorptive separation of benzene, cyclohexene, and cyclohexane by amorphous nonporous amide naphthotube solids. *Angew. Chem., Int. Ed.* **2020**, *59*, 19945–19950.
- (52) Sun, S.; Hu, X.-Y.; Chen, D.; Shi, J.; Dong, Y.; Lin, C.; Pan, Y.; Wang, L. Pillar [5] arene-based side-chain polypseudorotaxanes as an anion-responsive fluorescent sensor. *Polym. Chem.* **2013**, *4*, 2224–2229.

- (53) Sun, S.; Shi, J.-B.; Dong, Y.-P.; Lin, C.; Hu, X.-Y.; Wang, L.-Y. A pillar [5] arene-based side-chain pseudorotaxanes and polypseudorotaxanes as novel fluorescent sensors for the selective detection of halogen ions. *Chin. Chem. Lett.* **2013**, *24*, 987–992.
- (54) Yu, G.; Zhang, Z.; Han, C.; Xue, M.; Zhou, Q.; Huang, F. A non-symmetric pillar [5] arene-based selective anion receptor for fluoride. *ChemComm.* **2012**, *48*, 2958–2960.
- (55) Nierengarten, I.; Nothisen, M.; Sigwalt, D.; Biellmann, T.; Holler, M.; Remy, J. S.; Nierengarten, J. F. Polycationic pillar [5] arene derivatives: Interaction with DNA and biological applications. *Eur. J. Chem.* **2013**, *19*, 17552–17558.
- (56) Han, C.; Zhao, D.; Dong, S. Host-Guest Complexations Between Pillar [6] arenes and Neutral Pentaerythritol Derivatives. *Chem.: Asian J.* **2020**, *15*, 2642–2645.
- (57) Hu, X.-Y.; Wu, X.; Duan, Q.; Xiao, T.; Lin, C.; Wang, L. Novel pillar [5] arene-based dynamic polypseudorotaxanes interlocked by the quadruple hydrogen bonding ureidopyrimidinone motif. *Org. Lett.* **2012**, *14*, 4826–4829.
- (58) Si, W.; Xin, P.; Li, Z.-T.; Hou, J.-L. Tubular unimolecular transmembrane channels: construction strategy and transport activities. *Acc. Chem. Res.* **2015**, *48*, 1612–1619.
- (59) Guo, S.; Song, Y.; He, Y.; Hu, X. Y.; Wang, L. Highly Efficient Artificial Light-Harvesting Systems Constructed in Aqueous Solution Based on Supramolecular Self-Assembly. *Angew. Chem., Int. Ed.* **2018**, *130*, 3217–3221.
- (60) Xiao, T.; Zhong, W.; Zhou, L.; Xu, L.; Sun, X.-Q.; Elmes, R. B.; Hu, X.-Y.; Wang, L. Artificial light-harvesting systems fabricated by supramolecular host-guest interactions. *Chin. Chem. Lett.* **2019**, *30*, 31–36.
- (61) Jie, K.; Zhou, Y.; Li, E.; Huang, F. Nonporous adaptive crystals of pillararenes. *Acc. Chem. Res.* **2018**, *51*, 2064–2072.
- (62) Xiao, T.; Xu, L.; Zhong, W.; Zhou, L.; Sun, X. Q.; Hu, X. Y.; Wang, L. Advanced functional materials constructed from pillar [n] arenes. *Isr. J. Chem.* **2018**, *58*, 1219–1229.
- (63) Xiao, T.; Xu, L.; Zhou, L.; Sun, X.-Q.; Lin, C.; Wang, L. Dynamic hydrogels mediated by macrocyclic host-guest interactions. *J. Mater. Chem. B* **2019**, *7*, 1526–1540.
- (64) Xiao, T.; Zhong, W.; Xu, L.; Sun, X. Q.; Hu, X. Y.; Wang, L. Supramolecular vesicles based on pillar[n]arenes: design, construction, and applications. *Org. Biomol. Chem.* **2019**, *17*, 1336–1350.
- (65) Yu, G.; Yu, W.; Shao, L.; Zhang, Z.; Chi, X.; Mao, Z.; Gao, C.; Huang, F. Fabrication of a Targeted Drug Delivery System from a Pillar[5]arene-Based Supramolecular Diblock Copolymeric Amphiphile for Effective Cancer Therapy. *Adv. Funct. Mater.* **2016**, *26*, 8999–9008.
- (66) Saleh, N.; Koner, A. L.; Nau, W. M. Activation and stabilization of drugs by supramolecular pKa shifts: drug-delivery applications tailored for cucurbiturils. *Angew. Chem., Int. Ed. Engl.* **2008**, *47*, 5398–5401.
- (67) Wang, R.; MacGillivray, B. C.; Macartney, D. H. Stabilization of the base-off forms of vitamin B12 and coenzyme B12 by encapsulation of thea-axial 5, 6-dimethylbenzimidazole ligand with cucurbit [7] uril. *Dalton Trans.* **2009**, *9*, 3584–3589.
- (68) Koner, A. L.; Ghosh, I.; Saleh, N.i.; Nau, W. M. Supramolecular encapsulation of benzimidazole-derived drugs by cucurbit[7]uril. *Can. J. Chem.* **2011**, *89*, 139–147.
- (69) Cheung, C.; Gonzalez, F. J. Humanized mouse lines and their application for prediction of human drug metabolism and toxicological risk assessment. *J. Pharmacol. Exp. Ther.* **2008**, *327*, 288–299.
- (70) Gould, M.; Nelson, L. M.; Waterer, D.; Hynes, R. K. Biocontrol of *Fusarium sambucinum*, dry rot of potato, by *Serratia plymuthica* 5–6. *Biocontrol Sci. Technol.* **2008**, *18*, 1005–1016.
- (71) Lahlali, R.; Massart, S.; De Clercq, D.; Serrhini, M. N.; Creemers, P.; Jijakli, M. H. Assessment of *Pichia anomala* (strain K) efficacy against blue mould of apples when applied pre-or post-harvest under laboratory conditions and in orchard trials. *Eur. J. Plant Pathol.* **2009**, *123*, 37–45.
- (72) Omar, I.; O'Neill, T.; Rossall, S. Biological control of *Fusarium crown and root rot* of tomato with antagonistic bacteria and integrated control when combined with the fungicide carbendazim. *Plant Pathol.* **2006**, *55*, 92–99.
- (73) Pourgholami, M. H.; Szwajcer, M.; Chin, M.; Liauw, W.; Seef, J.; Galetti, P.; Morris, D. L.; Links, M. Phase I clinical trial to determine maximum tolerated dose of oral albendazole in patients with advanced cancer. *Cancer chemotherapy and pharmacology.* **2010**, *65*, 597–605.
- (74) Schirra, M.; D'Aquino, S.; Palma, A.; Angioni, A.; Cabras, P. Factors affecting the synergy of thiabendazole, sodium bicarbonate, and heat to control postharvest green mold of citrus fruit. *J. Agric. Food Chem.* **2008**, *56*, 10793–10798.
- (75) Erspamer, V.; Asero, B. Identification of Enteramine, the Specific Hormone of the Enterochromaffin Cell System, as 5-Hydroxytryptamine. *Nature* **1952**, *169*, 800–801.
- (76) Walther, D. J.; Peter, J.-U.; Bashammakh, S.; Hörtnagl, H.; Voits, M.; Fink, H.; Bader, M. Synthesis of Serotonin by a Second Tryptophan Hydroxylase Isoform. *Science* **2003**, *299*, 76.
- (77) Voet, D.; Voet, J. G.; Pratt, C. W. *Fundamentals of biochemistry: Life at the molecular level*, 5th ed.; John Wiley & Sons: New York, 2016; pp 245–292.
- (78) Kishi, T.; Tanaka, M.; Tanaka, J. Electronic Absorption and Fluorescence Spectra of 5-Hydroxytryptamine (Serotonin). Protonation in the Excited State. *Bull. Chem. Soc. Jpn.* **1977**, *50*, 1267–1271.
- (79) Chandra, F.; Dutta, T.; Koner, A. L. Supramolecular Encapsulation of a Neurotransmitter Serotonin by Cucurbit[7]uril. *Front Chem.* **2020**, *8*, 582757.
- (80) Liu, J.; Wang, T.; Wang, X.; Luo, L.; Guo, J.; Peng, Y.; Xu, Q.; Miao, J.; Zhang, Y.; Ling, Y. Development of novel β -carboline-based hydroxamate derivatives as HDAC inhibitors with DNA damage and apoptosis inducing abilities. *MedChemComm.* **2017**, *8*, 1213–1219.
- (81) Pari, K.; Sundari, C. S.; Chandani, S.; Balasubramanian, D. β -Carbolines that accumulate in human tissues may serve a protective role against oxidative stress. *J. Biol. Chem.* **2000**, *275*, 2455–2462.
- (82) Zhao, J.-Q.; Wang, Y.-M.; Yang, Y.-L.; Zeng, Y.; Wang, Q.-L.; Shao, Y.; Mei, L.-J.; Shi, Y.-P.; Tao, Y.-D. Isolation and identification of antioxidant and α -glucosidase inhibitory compounds from fruit juice of *Nitraria tangutorum*. *Food Chem.* **2017**, *227*, 93–101.
- (83) Bloom, H.; Barchas, J.; Sandler, M.; Usdin, E. *Progress in Clinical and Biological Research. Beta-carbolines and Tetrahydroisoquinolines*; Alan R. Liss Inc.: New York, 1982; pp 428.
- (84) Vignoni, M.; Rasse-Suriani, F. A.; Butzbach, K.; Erra-Balsells, R.; Epe, B.; Cabrerizo, F. M. Mechanisms of DNA damage by photoexcited 9-methyl- β -carbolines. *Org. Biomol. Chem.* **2013**, *11*, 5300–5309.
- (85) Paul, B. K.; Ghosh, N.; Mondal, R.; Mukherjee, S. Contrasting effects of salt and temperature on niosome-bound norharmane: direct evidence for positive heat capacity change in the niosome: β -cyclodextrin interaction. *J. Phys. Chem. B* **2016**, *120*, 4091–4101.
- (86) Assaf, K. I.; Alnajjar, M. A.; Nau, W. M. Supramolecular assemblies through host-guest complexation between cucurbiturils and an amphiphilic guest molecule. *ChemComm.* **2018**, *54*, 1734–1737.
- (87) Ghosh, I.; Nau, W. M. The strategic use of supramolecular pKa shifts to enhance the bioavailability of drugs. *Adv. Drug Delivery Rev.* **2012**, *64*, 764–783.
- (88) Lamounier, A.; Mateus, N.; da Cunha, A.; Luna, A.; Aucélio, R. Determination of six β -carboline alkaloids in urine and phytotherapeutic extracts using micellar liquid chromatography with fluorimetric detection. *J. Liq. Chromatogr. Relat. Technol.* **2015**, *38*, 997–1006.
- (89) Chandra, F.; Kumar, P.; Koner, A. L. Encapsulation and modulation of protolytic equilibrium of beta-carboline-based norharmane drug by cucurbit[7]uril and micellar environments for

- enhanced cellular uptake. *Colloids Surf. B Biointerfaces*. **2018**, *171*, 530–537.
- (90) Wang, R.; Yuan, L.; Macartney, D. H. A green to blue fluorescence switch of protonated 2-aminoanthracene upon inclusion in cucurbit [7] uril. *ChemComm*. **2005**, *67*, 5867–5869.
- (91) Pluth, M. D.; Bergman, R. G.; Raymond, K. N. Making amines strong bases: Thermodynamic stabilization of protonated guests in a highly-charged supramolecular host1. *J. Am. Chem. Soc.* **2007**, *129*, 11459–11467.
- (92) Boulikas, T.; Vougiouka, M. Cisplatin and platinum drugs at the molecular level. (Review). *Oncol. Rep.* **2003**, *10*, 1663–1682.
- (93) Piccart, M. J.; Lamb, H.; Vermorken, J. B. Current and future potential roles of the platinum drugs in the treatment of ovarian cancer. *Ann. Oncol.* **2001**, *12*, 1195–1203.
- (94) Wong, E.; Giandomenico, C. M. Current status of platinum-based antitumor drugs. *Chem. Rev.* **1999**, *99*, 2451–2466.
- (95) Hartmann, J. T.; Lipp, H.-P. Toxicity of platinum compounds. *Expert Opin Pharmacother.* **2003**, *4*, 889–901.
- (96) Farrell, N. Polynuclear Charged Platinum Compounds as a New Class of Anticancer Agents. In *Platinum-Based Drugs in Cancer Therapy*; Kelland, L. R., Farrell, N. P., Eds.; Humana Press: Totowa, NJ, 2000; pp 321–338.
- (97) Lippert, B.; Chemistry and biochemistry of a leading anticancer drug, *Verlag Helv. Chim. Acta: Zürich* **1999**.
- (98) Calvert, A.; Thomas, H.; Colombo, N.; Gore, M.; Earl, H.; Sena, L.; Camboni, G.; Liati, P.; Sessa, C. Phase II clinical study of BBR 3464, a novel, bifunctional platinum analogue. in patients with advanced ovarian cancer. *Eur. J. Cancer*. **2001**, *37*, S260–S260.
- (99) Wheate, N. J.; Buck, D. P.; Day, A. I.; Collins, J. G. Cucurbit [n] uril binding of platinum anticancer complexes. *Dalton Trans.* **2006**, 451–458.
- (100) Wheate, N. J.; Day, A. I.; Blanch, R. J.; Arnold, A. P.; Cullinane, C.; Collins, J. G. Multi-nuclear platinum complexes encapsulated in cucurbit[n]uril as an approach to reduce toxicity in cancer treatment. *Chem. Commun.* **2004**, 1424–1425.
- (101) Wheate, N. J.; Buck, D. P.; Day, A. I.; Collins, J. G. Cucurbit[n]uril binding of platinum anticancer complexes. *Dalton Trans.* **2006**, 451–458.
- (102) Brogden, R. N.; Carmine, A. A.; Heel, R. C.; Speight, T. M.; Avery, G. S. Ranitidine: A Review of its Pharmacology and Therapeutic Use in Peptic Ulcer Disease and Other Allied Diseases. *Drugs* **1982**, *24*, 267–303.
- (103) Grant, S. M.; Langtry, H. D.; Brogden, R. N. Ranitidine. *Drugs* **1989**, *37*, 801–870.
- (104) Wang, R.; Macartney, D. H. Cucurbit[7]uril host-guest complexes of the histamine H₂-receptor antagonist ranitidine. *Org. Biomol. Chem.* **2008**, *6*, 1955–1960.
- (105) Dumanović, D.; Juranić, I.; Dželetović, D.; Vasić, V. M.; Jovanović, J. Protolytic constants of nizatidine, ranitidine and N,N'-dimethyl-2-nitro-1,1-ethenediamine; spectrophotometric and theoretical investigation. *J. Pharm. Biomed* **1997**, *15*, 1667–1678.
- (106) Hohnjec, M.; Rendic, S.; Alebickolbah, T.; Kajfez, F.; Blazevic, N.; Kufnec, J. Physical and spectroscopic data of ranitidine. *Acta Pharm. Jugoslav.* **1981**, *31*, 131–142.
- (107) Crisponi, G.; Cristiani, F.; Nurchi, V. M.; Silvagni, R.; Ganadu, M. L.; Lubinu, G.; Naldini, L.; Panzanelli, A. A potentiometric, spectrophotometric and ¹H NMR study on the interaction of cimetidine, famotidine and ranitidine with platinum-(II) and palladium(II) metal ions. *Polyhedron* **1995**, *14*, 1517–1530.
- (108) Hempel, A.; Camerman, N.; Mastropaolo, D.; Camerman, A. Ranitidine hydrochloride, a polymorphic crystal form. *Acta Crystallogr. Sec C: Cryst. Str. Commun.* **2000**, *56*, 1048–1049.
- (109) Ishida, T.; In, Y.; Inoue, M. Structure of ranitidine hydrochloride. *Acta Crystallogr. Sec C: Cryst. Str. Commun.* **1990**, *46*, 1893–1896.
- (110) Mirmehrabi, M.; Rohani, S. An approach to solvent screening for crystallization of polymorphic pharmaceuticals and fine chemicals. *J. Pharm. Sci.* **2005**, *94*, 1560–1576.
- (111) Teraoka, R.; Otsuka, M.; Matsuda, Y. Effects of temperature and relative humidity on the solid-state chemical stability of ranitidine hydrochloride. *J. Pharm. Sci.* **1993**, *82*, 601–604.
- (112) Haywood, P. A.; Martin-Smith, M.; Cholerton, T. J.; Evans, M. B. Isolation and identification of the hydrolytic degradation products of ranitidine hydrochloride. *J. Chem. Soc., Perkin trans.* **1987**, *1*, 951–954.
- (113) Evans, M. B.; Haywood, P. A.; Johnson, D.; Martin-Smith, M.; Munro, G.; Wahlich, J. C. Chromatographic methods for determining the identity, strength and purity of ranitidine hydrochloride both in the drug substance and its dosage form—an exercise in method selection, development, definition and validation. *J. Pharm. Biomed* **1989**, *7*, 1–22.
- (114) Langston, J. W.; Ballard, P.; Tetrad, J. W.; Irwin, I. Chronic Parkinsonism in Humans Due to a Product of Meperidine-Analog Synthesis. *Science* **1983**, *219*, 979–980.
- (115) Lin, M. T.; Beal, M. F. Mitochondrial dysfunction and oxidative stress in neurodegenerative diseases. *Nature* **2006**, *443*, 787–795.
- (116) Li, S.; Chen, H.; Yang, X.; Bardelang, D.; Wyman, I. W.; Wan, J.; Lee, S. M. Y.; Wang, R. Supramolecular Inhibition of Neurodegeneration by a Synthetic Receptor. *ACS Med. Chem. Lett.* **2015**, *6*, 1174–1178.
- (117) Hare, D. J.; Adlard, P. A.; Doble, P. A.; Finkelstein, D. I. Metallobiology of 1-methyl-4-phenyl-1,2,3,6-tetrahydropyridine neurotoxicity. *Metallomics* **2013**, *5*, 91–109.
- (118) Smeyne, R. J.; Jackson-Lewis, V. The MPTP model of Parkinson's disease. *Mol. Brain Res.* **2005**, *134*, 57–66.
- (119) Mallick, S.; Pal, K.; Koner, A. L. Probing microenvironment of micelle and albumin using diethyl 6-(dimethylamino) naphthalene-2, 3-dicarboxylate: An electroneutral solvatochromic fluorescent probe. *J. Colloid Interface Sci.* **2016**, *467*, 81–89.
- (120) Chandra, F.; Pal, K.; Lathwal, S.; Koner, A. L. Supramolecular guest relay using host-protein nanocavities: an application of host-induced guest protonation. *Mol. Biosyst.* **2016**, *12*, 2859–2866.
- (121) Uzunova, V. D.; Cullinane, C.; Brix, K.; Nau, W. M.; Day, A. I. Toxicity of cucurbit[7]uril and cucurbit[8]uril: an exploratory in vitro and in vivo study. *Org. Biomol. Chem.* **2010**, *8*, 2037–2042.
- (122) Barbera, L.; Franco, D.; De Plano, L. M.; Gattuso, G.; Guglielmino, S. P.; Lentini, G.; Manganaro, N.; Marino, N.; Pappalardo, S.; Parisi, M. F.; et al. A water-soluble pillar [5] arene as a new carrier for an old drug. *Org. Biomol. Chem.* **2017**, *15*, 3192–3195.
- (123) Hao, Q.; Chen, Y.; Huang, Z.; Xu, J.-F.; Sun, Z.; Zhang, X. Supramolecular chemotherapy: carboxylated pillar [6] arene for decreasing cytotoxicity of oxaliplatin to normal cells and improving its anticancer bioactivity against colorectal cancer. *ACS Appl. Mater. Interfaces* **2018**, *10*, 5365–5372.
- (124) Li, B.; Meng, Z.; Li, Q.; Huang, X.; Kang, V.; Dong, H.; Chen, J.; Sun, J.; Dong, Y.; Li, J.; et al. A pH responsive complexation-based drug delivery system for oxaliplatin. *Chem. Sci.* **2017**, *8*, 4458–4464.
- (125) Yang, K.; Wen, J.; Chao, S.; Liu, J.; Yang, K.; Pei, Y.; Pei, Z. A supramolecular photosensitizer system based on the host-guest complexation between water-soluble pillar [6] arene and methylene blue for durable photodynamic therapy. *ChemComm* **2018**, *54*, 5911–5914.
- (126) Feng, W.; Jin, M.; Yang, K.; Pei, Y.; Pei, Z. Supramolecular delivery systems based on pillararenes. *ChemComm* **2018**, *54*, 13626–13640.
- (127) Chang, Y.; Yang, K.; Wei, P.; Huang, S.; Pei, Y.; Zhao, W.; Pei, Z. Cationic vesicles based on amphiphilic pillar [5] arene capped with ferrocenium: a redox-responsive system for drug/siRNA co-delivery. *Angew. Chem., Int. Ed.* **2014**, *53*, 13126–13130.
- (128) Yu, G.; Xue, M.; Zhang, Z.; Li, J.; Han, C.; Huang, F. A water-soluble pillar [6] arene: synthesis, host-guest chemistry, and its application in dispersion of multiwalled carbon nanotubes in water. *J. Am. Chem. Soc.* **2012**, *134*, 13248–13251.

- (129) Duan, Q.; Cao, Y.; Li, Y.; Hu, X.; Xiao, T.; Lin, C.; Pan, Y.; Wang, L. pH-responsive supramolecular vesicles based on water-soluble pillar [6] arene and ferrocene derivative for drug delivery. *J. Am. Chem. Soc.* **2013**, *135*, 10542–10549.
- (130) Qu, D.-H.; Wang, Q.-C.; Zhang, Q.-W.; Ma, X.; Tian, H. Photoresponsive host-guest functional systems. *Chem. Rev.* **2015**, *115*, 7543–7588.
- (131) Xia, D.; Yu, G.; Li, J.; Huang, F. Photo-responsive self-assembly based on a water-soluble pillar [6] arene and an azobenzene-containing amphiphile in water. *ChemComm* **2014**, *50*, 3606–3608.
- (132) Wu, X.; Li, Y.; Lin, C.; Hu, X.-Y.; Wang, L. GSH-and pH-responsive drug delivery system constructed by water-soluble pillar [5] arene and lysine derivative for controllable drug release. *ChemComm* **2015**, *51*, 6832–6835.
- (133) Hu, X.-Y.; Liu, X.; Zhang, W.; Qin, S.; Yao, C.; Li, Y.; Cao, D.; Peng, L.; Wang, L. Controllable Construction of Biocompatible Supramolecular Micelles and Vesicles by Water-Soluble Phosphate Pillar[5,6]arenes for Selective Anti-Cancer Drug Delivery. *Chem. Mater.* **2016**, *28*, 3778–3788.
- (134) Cao, Y.; Hu, X.-Y.; Li, Y.; Zou, X.; Xiong, S.; Lin, C.; Shen, Y.-Z.; Wang, L. Multistimuli-responsive supramolecular vesicles based on water-soluble pillar [6] arene and SAINT complexation for controllable drug release. *J. Am. Chem. Soc.* **2014**, *136*, 10762–10769.
- (135) Jie, K.; Zhou, Y.; Yao, Y.; Shi, B.; Huang, F. CO₂-responsive pillar [5] arene-based molecular recognition in water: establishment and application in gas-controlled self-assembly and release. *J. Am. Chem. Soc.* **2015**, *137*, 10472–10475.
- (136) Meng, L.-B.; Li, D.; Xiong, S.; Hu, X.-Y.; Wang, L.; Li, G. FRET-capable supramolecular polymers based on a BODIPY-bridged pillar[5]arene dimer with BODIPY guests for mimicking the light-harvesting system of natural photosynthesis. *ChemComm* **2015**, *51*, 4643–4646.
- (137) Wu, X.; Gao, L.; Hu, X. Y.; Wang, L. Supramolecular Drug Delivery Systems Based on Water-Soluble Pillar [n] arenes. *Chem. Rec.* **2016**, *16*, 1216–1227.
- (138) Cao, Y.; Li, Y.; Hu, X.-Y.; Zou, X.; Xiong, S.; Lin, C.; Wang, L. Supramolecular Nanoparticles Constructed by DOX-Based Prodrug with Water-Soluble Pillar[6]arene for Self-Catalyzed Rapid Drug Release. *Chem. Mater.* **2015**, *27*, 1110–1119.
- (139) Yang, K.; Chang, Y.; Wen, J.; Lu, Y.; Pei, Y.; Cao, S.; Wang, F.; Pei, Z. Supramolecular vesicles based on complex of trp-modified pillar [5] arene and galactose derivative for synergistic and targeted drug delivery. *Chem. Mater.* **2016**, *28*, 1990–1993.
- (140) Nierengarten, I.; Buffet, K.; Holler, M.; Vincent, S. P.; Nierengarten, J.-F. A mannosylated pillar [5] arene derivative: chiral information transfer and antiadhesive properties against uropathogenic bacteria. *Tetrahedron Lett.* **2013**, *54*, 2398–2402.
- (141) Yu, G.; Ma, Y.; Han, C.; Yao, Y.; Tang, G.; Mao, Z.; Gao, C.; Huang, F. A sugar-functionalized amphiphilic pillar [5] arene: synthesis, self-assembly in water, and application in bacterial cell agglutination. *J. Am. Chem. Soc.* **2013**, *135*, 10310–10313.
- (142) Yang, K.; Chang, Y.; Wen, J.; Lu, Y.; Pei, Y.; Cao, S.; Wang, F.; Pei, Z. Supramolecular Vesicles Based on Complex of Trp-Modified Pillar[5]arene and Galactose Derivative for Synergistic and Targeted Drug Delivery. *Chem. Mater.* **2016**, *28*, 1990–1993.
- (143) Gao, L.; Wang, T.; Jia, K.; Wu, X.; Yao, C.; Shao, W.; Zhang, D.; Hu, X.-Y.; Wang, L. Glucose-Responsive Supramolecular Vesicles Based on Water-Soluble Pillar[5]arene and Pyridylboronic Acid Derivatives for Controlled Insulin Delivery. *Eur. J. Chem.* **2017**, *23*, 6605–6614.
- (144) Zuo, M.; Qian, W.; Xu, Z.; Shao, W.; Hu, X.-Y.; Zhang, D.; Jiang, J.; Sun, X.; Wang, L. Multiresponsive Supramolecular Theranostic Nanoplatform Based on Pillar[5]arene and Diphenylboronic Acid Derivatives for Integrated Glucose Sensing and Insulin Delivery. *Small* **2018**, *14*, 1801942.
- (145) Jeon, Y. J.; Kim, S.-Y.; Ko, Y. H.; Sakamoto, S.; Yamaguchi, K.; Kim, K. Novel molecular drug carrier: encapsulation of oxaliplatin in cucurbit [7] uril and its effects on stability and reactivity of the drug. *Org. Biomol. Chem.* **2005**, *3*, 2122–2125.
- (146) Hettiarachchi, G.; Nguyen, D.; Wu, J.; Lucas, D.; Ma, D.; Isaacs, L.; Briken, V. Toxicology and drug delivery by cucurbit [n] uril type molecular containers. *PLoS One* **2010**, *5*, No. e10514.
- (147) Wu, J.-R.; Wu, G.; Yang, Y.-W. Pillararene-Inspired Macrocycles: From Extended Pillar[n]are to Geminiarenes. *Acc. Chem. Res.* **2022**, *55*, 3191–3204.